WPI

Solid Acid Catalysts for Cellulose Hydrolysis: Structural Investigations Into the Thermal Stability and Catalytic Mechanism of Chloromethyl Polystyrene Based Solid Acid Catalysts

A Major Qualifying Project Submitted to the Faculty of

Worcester Polytechnic Institute

in partial fulfillment of the requirements for the

Degree of Bachelor of Science

in

Chemical Engineering

By:
Jordan Finzel

Advisor:
Professor Michael Timko

With Special Assistance From:
Maksim Tyufekchiev

4/23/18

Table of Contents

Abstract

Cellulose is a highly abundant biopolymer contained within “woody” biomass that offers a sustainable carbon alterative to fossil fuels. Current options for treatment of cellulose to produce favorable products such as glucose and levulinic acid include either enzymatic hydrolysis of dilute-acid hydrolysis. Limitations of these two approaches include slow reaction rates, corrosive conditions, and recyclability issues due to difficult separations, all of which increase the cost of the process. Solid acid catalysts have been posed as a viable pretreatment option that could potentially overcome these limitations.

A popular catalyst for this reaction is (chloromethyl)polystyrene (CMP) and its sulfonated derivates.. These catalysts have been reported to mechanistically hydrolyze cellulose in a similar fashion to cellulase enzymes. A serious mechanistic study has yet to provide details into the kinetics of this catalysis.

This work demonstrates that the solid acid actually leaches chloride anions over time, forming aqueous hydrochloric acid *in-situ*. The release of acid followed first order kinetics, and therefore the $[H^+]$ concentration could be modeled as a function of time. Kinetic modeling using literature parameters for liquid acid catalyzed cellulose hydrolysis was employed in conjunction with the time-dependent $[H^+]$ concentration. A Monte Carlo method was used to capture experimental uncertainties of $[H^+]$ concentration and temperature within the kinetic model.

Experimental cellulose hydrolysis data had good agreement with the liquid acid catalyzed kinetic model. This suggests that the predominating kinetic mechanism is actually catalyzed by a homogenous liquid acid being leached over. The catalytic effects of the solid acid catalyst itself are unclear.

Acknowledgments

I would like to thank Professor Michal Timko of the Department of Chemical Engineering at Worcester Polytechnic Institute for the opportunity to work together on this project. His support and insight was invaluable and his mentoring allowed me the freedom to develop the project as I saw fit.

Additionally, I would like to thank PhD candidate Maksim Tyufekchiev for his continuous assistance both experimentally and intellectually. This project would not have been possible without his groundwork over the previous years, coupled with his guidance in the lab on technical matters and on elucidating the defining science behind our observations.

I would also like to thank Environmental Lab Manager Wenwen Yao of the Civil and Environmental Engineering Department at Worcester Polytechnic Institute for here availability and willingness to assist with sample analysis as well as Tom Partington, Machinist from the Goddard Hall Machine Shop for his time and assistance.

Lastly, I would like to thank the National Science Foundation for the funding of this project via Grant #1554283, awarded to Professor Timko.

Chapter 1: Introduction

Bioproducts have become an intensive area of research and development because they offer a sustainable alternative to petroleum based products. In 2016, 97 million barrels of liquid fuels were consumed daily on a global scale and projections have this number trending upwards in the years to come.[1] Equally important is the global use of commercial chemicals, of which sales have increased over 200% from 2005 to 2015.[2] These petroleum based products have led to the increased release of carbon species into the environment and have upset the natural carbon cycle. Consequentially, atmospheric greenhouse gas concentrations have increased unprecedentedly by nearly 40% over the past 250 years which has contributed to the rise of average global temperatures by 2-5°C, ocean acidification, and climate change that carries concerns environmentally, politcally, and socially.[3] Clearly, a more sustainable method of meeting our energy and material demands is of paramount importance.

While producing fuels and widely used commercial chemicals in a more sustainable manner poses a great challenge, solutions could potentially have global implications. Bioproducts produced from biomass offer a more sustainable route to meeting our material needs that could lead to greater energy independence, reduce greenhouse gas emissions, and offer a greater diversity of platform chemicals.[4] Traditionally, conversion of biomass to bioproducts has been separated into two generic platforms; thermochemical routes and biochemical routes, both of which pose different challenges.

---

[1] U.S Energy Information Administration. "Short-Term Energy Outlook (STEO) Forecast Highlights." (2017): n. pag. Print.

[2] Cefic. "Facts and Figures of the European Chemical Industry 2016." (2016): n. pag. Print.

[3] Zalasiewicz, Jan et al. "The New World of the Anthropocene." *Environmental Science & Technology* 44.7 (2010): 2228–2231. Print.

[4] Hoekman, S. Kent. "Biofuels in the U.S. - Challenges and Opportunities." *Renewable Energy* 34.1 (2009): 14–22. Web.

Thermochemical routes are often limited by their selectivity. While they are adaptable to using multiple types of feedstocks, it is difficult to selctively convert biomass into a specific product. In order for more selective conversion, high pressures and temperatures (at times in excess of 3,500 psi and 1200°C), are used to gain greater control of the system.[5] These high temperature and high pressure conditions are energy intensive and limit the over efficiency of the processes. Consequentially, producing bioproducts via the thermochemical route can sometimes be limited in the overall sustainability of the process, at times even be net energy intensive for the desired conversions.

Analyses have shown that while currently biochemical pathways are less efficient than their thermochemical counterparts, the biochemical platform has the potential for overall higher efficiencies.[6] Despite this, the biochemical platform poses it's own challenges, mainly difficulty in dealing with the diverse nature of biomass feedstocks.[4] Consequentially, biomass raw materials must go through an extensive pretreatment process prior to being used in any biochemical pathway that would result in the generation of desirable bioproducts. In order for enzymatic (biochemical) pretreatments to be effective, a cocktail of up to 50 different enzymes must be used to succesfully convert biomass into usable sugars.[7] As a result, the main motive for research in the biochemical platform is developing enzymatic hydrolysis to the point that it can be cost competitive with other technologies.[8]

Techno-economic analysis suggest that even in the case of highly developed lignocellulosic to ethanol conversion, pretreatment costs and associated seperations

---

[5] Nielsen, Rudi P., Göran Olofsson, and Erik G. Søgaard. "CatLiq - High Pressure and Temperature Catalytic Conversion of Biomass: The CatLiq Technology in Relation to Other Thermochemical Conversion Technologies." *Biomass and Bioenergy* 39 (2012): 399–402. Web.

[6] Fendt, Sebastian et al. "Comparison of Synthetic Natural Gas Production Pathways for the Storage of Renewable Energy." *Wiley Interdisciplinary Reviews: Energy and Environment* 5.3 (2016): 327–350. Web.

[7] Balan, Venkatesh. "Current Challenges in Commercially Producing Biofuels from Lignocellulosic Biomass." *ISRN Biotechnology* 2014.i (2014): 1–31. Web.

[8] Hong, Yan et al. "Impact of Cellulase Production on Environmental and Financial Metrics for Lignocellulosic Ethanol." *Biofuels, Bioproducts and Biorefining* 7.3 303–313. Web.

account for over a third of the total process costs.[9] The need for cost effective pretreatment processes, namely the selective hydrolysis of cellulose, therefore represents a critical step in the process of sustainable production of bioproducts from biomass.[10] Current practices for the hydrolysis of cellulose include enzymatic hydrolysis as well as acid catalyzed hydrolysis. While enymatic hydrolysis can be carried out at mild temperatures with high selectivity towards favorable products (glucose), drawbacks include limitations as to the rate of the process. Acid catalyzed hydrolysis must be carried out at higher temperatures which restricts selectivity and requires greater energy inputs, and also inherintly requires harsher, more corrosive conditions.[11] Additionally, both of these methods require further seperatations, and are cost prohibitive when trying to implement on an industrial scale.[6-8]

It is apparent that an optimized pretreatment process for the hydrolysis of cellulose to glucose could potentially alter the current landscape of sustainably producing bioproducts from biomass. Ideally, the process would be able to be carried out at low temperatures with selective conversion to glucose, or potentially levulinic acid, in high yields. An attractive option that has received attention recently is the use of solid acid catalysts, which have the added benefit of reducing separation costs and could potentially be recovered and reused continuously.[12]

In particular, cellulase mimetic solid acid catalysts have shown promise. Cellulase mimetic catalysts are categorized as such because they are thought to

---

[9] Humbird, D. et al. "Process Design and Economics for Biochemical Conversion of Lignocellulosic Biomass to Ethanol: Dilute-Acid Pretreatment and Enzymatic Hydrolysis of Corn Stover." *Renewable Energy* 303.May (2011): 147. Web.

[10] Rinaldi, Roberto, and Ferdi Schuth. "Acid Hydrolysis of Cellulose as the Entry Point into Biorefinery Schemes." *ChemSusChem* 2.12 (2009): 1096–1107. Web. 5 Oct. 2017.

[11] Chaturvedi, Venkatesh, and Pradeep Verma. "An Overview of Key Pretreatment Processes Employed for Bioconversion of Lignocellulosic Biomass into Biofuels and Value Added Products." *3 Biotech* 3.5 (2013): 415–431. Web.

[12] Huang, Yao-Bing, and Yao Fu. "Hydrolysis of Cellulose to Glucose by Solid Acid Catalysts." *Green Chem.* 15.5 (2013): 1095–1111. Web.

catalyze the cleavage of the 1,4-beta-D-glycosidic linkages in cellulose in a similar fashion to cellulases.[13] The exact mechanism by which these catalysts act is not clear and is of particular interest. With an understanding of the kinetics and the catalytic mechanism for this reaction, rational catalyst design is possible to improve efficiency and possibly selectivity.

In this project, the thermostability and kinetics of popular cellulose mimetic solid acid, (chloromethyl)polystyrene (CMP) and sulfonated CMP derivatives, were investigated. Experimentally, these catalysts were subjected to reaction-like conditions and structural changes were investigated, specifically looking at how the functional groups, supposedly responsible for catalytic activity, changed. Additionally, computational kinetic modeling was performed to gauge the level of catalytic activity for these solid acids.

In the subsequent chapters, the background literature is reviewed, the research methodology and approach are laid out, and the results are presented with relevant discussion and conclusions. In the next chapter, a greater background on the overall problem of sustainability is discussed, along with how biomass has the potential to be a sustainable options, major barriers to using biomass for biofuels and bioproducts, how solid acid catalysts can address these barriers, and finally what studies have been conducted investigating polystyrene based solid acid catalysts and kinetic modeling.

---

[13] Shuai, Li, and Xuejun Pan. "Hydrolysis of Cellulose by Cellulase-Mimetic Solid Catalyst." *Energy & Environmental Science* 5.5 (2012): 6889. Web.

Chapter 2: Background

It is apparent that meeting our current energy and material needs is currently unsustainable. While new oil deposits and an excess of natural gas have temporarily alleviated the fear of running out of fossil fuels in the immediate future, the search for alternative forms of energy is still imperative. The uneven distribution of fossil fuel resources around the world has caused extensive political strife and will continue to cause both social and geopolitical problems so long as economies are dependent on fossil fuels.[14]

These problems aside, the negative environmental impacts of the combustion and rapid consumption of fossil fuel products is being felt globally. Erosion and sedimentation rates have increase by ten-fold, atmospheric greenhouse gas concentrations have increased unprecedentedly by nearly 40% over the past 250 years which has contributed to the rise of average global temperatures by 2-5°C as well as ocean acidification, not barring to mention that the current species extinction rate is on the order of magnitude of 1000 times the normal background rate.[3] Additional studies have shown with overwhelming consensus that these ecological phenomena can be directly attributed to human actions.[15] The most concerning direct effect of fossil fuel combustion, that has permeating secondary effects, is the release of greenhouse gasses, such as CO_2, into the atmosphere.

The largest source of anthropogenic greenhouse gas emmisions comes from the release of carbon dioxide during the combustion of fossil fuels.[16] Our usage of fossil fuels is disturbing the balance between the natural carbon cycle of the earth. As we produce more carbon dioxide by removing carbon rich sources stored within the earth, we effectively release carbon species into the environment adding inputs

---

[14] Scott, David Sanborn. "Fossil Sources: 'running Out' is Not the Problem." *International Journal of Hydrogen Energy* 30.1 (2005): 1–7. Web.

[15] Höök, Mikael, and Xu Tang. "Depletion of Fossil Fuels and Anthropogenic Climate Change-A Review." *Energy Policy* 52 (2013): 797–809. Web.

to the carbon cycle. The natural carbon sinks (i.e. forests, plants) can not keep up with this influx of carbon, and thus the anthropogenic carbon release has outpaced the natural carbon cycle.[16] The disrupted carbon cycle is shown below in Figure 1.

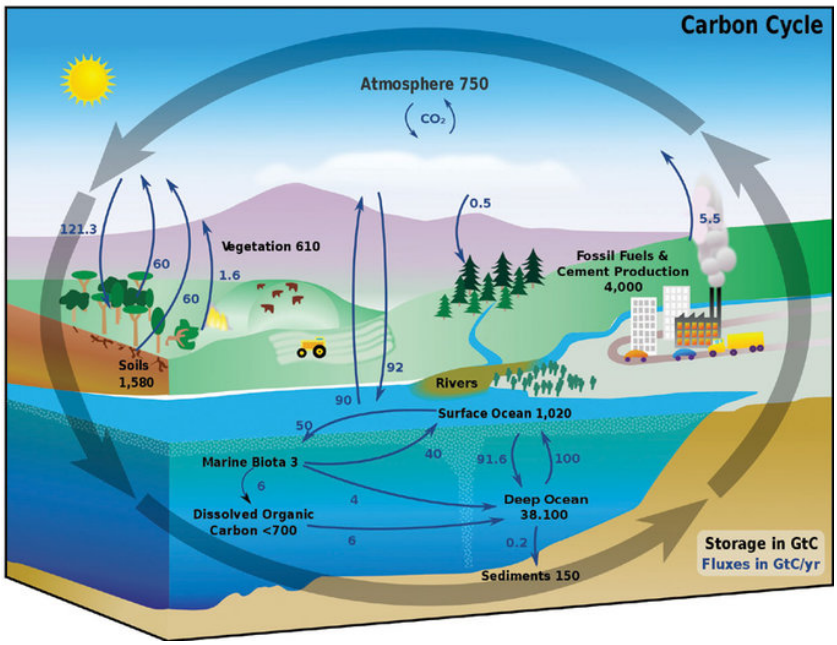

Figure 1: Carbon cycle with combustion of fossil fuels adding and storing significant amounts of carbon based greenhouse gasses.[17]

The need for alternative energy sources is paramount. Research is actively being conducted to make use of all renewable inputs including solar, wind, hydroelectric, geothermal, and others. Biomass has jumped out as an attractive and sustainable option, and will be discussed in the upcoming section.

2.1 Biomass for a Sustainable Future

Biomass is an attractive option for multiple reasons. First and foremost, use of biomass can help reduce the accumulation of anthropogenic carbon dioxide. As discussed previously, fossil fuels add a flux to the carbon cycle, and result in a net

[16] Olah, George A., G. K.Surya Prakash, and Alain Goeppert. "Anthropogenic Chemical Carbon Cycle for a Sustainable Future." *Journal of the American Chemical Society* 133.33 (2011): 12881–12898. Web.

[17] "The Carbon Cycle in the Earth System." Max Planck Society, www.mpg.de/19314/carbon_cycle.

accumulation. Adoption of biomass results in more land usage dedicated to carbon sinks such as forests and crop fields. Plants then take gaseous carbon from the air and turn it into oxygenated hydrocarbon materials. At the cost of conversion, this carbon can directly substitute in for transportation fuels and other petrochemical derivatives the world economy is currently based on. This closed carbon cycle is demonstrated below in Figure 2.

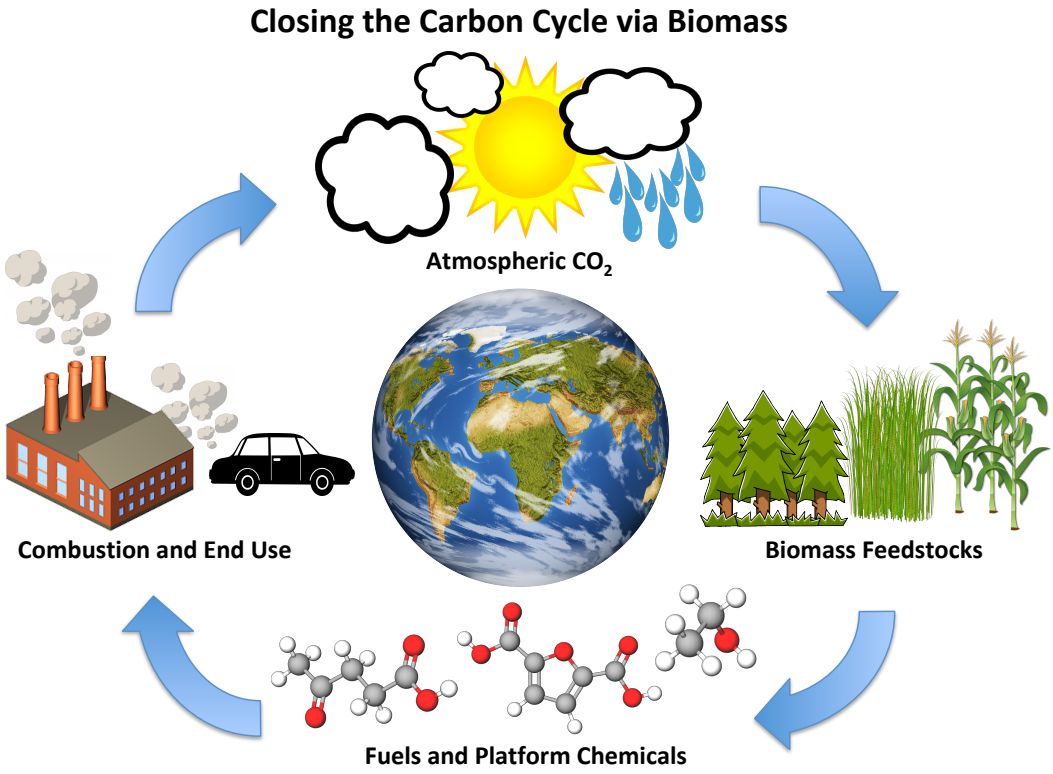

Figure 2: A closed carbon cycle based on the use of biomass.

All renewable energy substitutes offer the positive of reducing carbon emissions. Unlike other renewable energy platforms however, biomass as the added benefit of potentially producing not just energy, but commodity and specialty chemicals as well.[18] The global demand for commercial chemicals sales increased

[18] "Biomass Energy Basics." Biomass Energy Basics | NREL, www.nrel.gov/workingwithus/re-biomass.html.

over 200% from 2005 to 2015.[2] Biomass has a number of innately interesting structures and thus have the possibility to be turned into a number of highly sought after chemicals. For example, the United States Department of Energy (DOE) identified 12 different chemicals that could be produced from biomass that have major sustainable economic implications if they can be produced in an efficient manner.[19]

Of the available platforms for renewable energy, biomass has been the most heavily utilized both historically and today. The most simple example of biomass utilization for energy generation is the use of wood fireplaces to for heating. More recently, the production of sugar rich crops (corn in the United States and sugarcane in Brazil) has been developed for the production of bioethanol as an additive in liquid transportation fuels. Figure 3 below shows that biomass made up 46% of all renewable energy consumed in the United States in 2016.

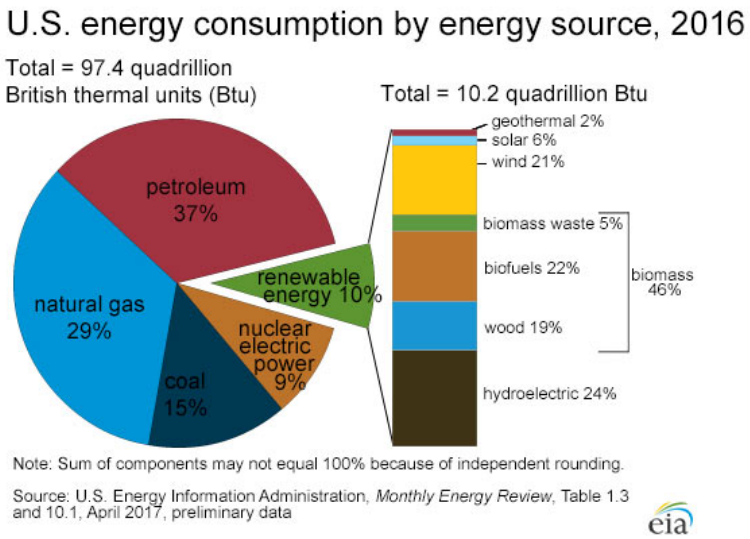

Figure 3: A break down of US energy consumption in 2016 showing biomass as the leading alternative energy source.[20]

---

[19] T, Werpy., and Petersen. G. "Top Value Added Chemicals from Biomass Volume I — Results of Screening for Potential Candidates from Sugars and Synthesis Gas Top Value Added Chemicals From Biomass Volume I : Results of Screening for Potential Candidates." 1 (2004): n. pag. Print.

[20] Renewable Energy Sources - Energy Explained, Your Guide To Understanding Energy - Energy Information Administration, www.eia.gov/energyexplained/?page=renewable_home.

Despite the high adoption of biomass as a current renewable resource, there has been a recent focus on making use of lignocellulosic biomass which presents a number of interesting but difficult challenges.

2.2 Lignocellulosic Biomass

The production of bioethanol from starchy sugars is a well-developed process. Second generation bioproducts are made from upgrading lignocellulosic biomass, which is the "woody" part of biomass that is often discarded and considred waste. This is an attractive option because it is making valuable fuels and chemicals from waste products, such as things like corn cobs and stalks as opposed to the starchy corn kernels themselves. While lignocellulosic biomass varies depending on source, composition consists mainly of cellulose (hexose sugars, 35–50%), hemicellulose (hexose and pentose sugars, 20–35%) and a remaining part lignin.[21] Of these components, cellulose is both the most abundant and most suitable for upgrading into more valuable products.

2.2.1 Structure of Cellulose

Cellulose is a highly abundant polymer present in all plant matter. It forms in linear chains without branching, and its rigidity is what gives plants their structure. Cellulose is insoluble in water and is a polymer consisting of beta-D-glucopyranose units, linked by (1→4) glycosidic bonds. A typical cellulose polymer has a degree of polymerization that ranges anywhere between 1,000 and 15,000, depending on the source of cellulose.[22] While the beta (1→4) glycosidic bonds are difficult to break, the glucose monomeric units of cellulose make it an attractive option for upgrading.

---

[21] Singh, Anoop et al. "Key Issues in Life Cycle Assessment of Ethanol Production from Lignocellulosic Biomass: Challenges and Perspectives." *Bioresource Technology* 101.13 (2010): 5003–5012. Web.

[22] OSullivan, A C. "Cellulose: The Structure Slowly Unravels." *Cellulose* 4.3 (1997): 173–207. Web.

2.2.1 Current Pretreatment Options

Cellulose clearly has potential as a renewable and abundant biopolymer, but difficulties in treating it and breaking it down present barriers to its implementation. There are essentially two methods currently implemented in the cellulose hydrolysis (decomposition of cellulose polymer into glucose units).

The first is the biochemical approach through enzymatic hydrolysis, using cellulase enzymes to hydrolyze the biopolymer. A major drawback with this approach is the lack of ability to deal with the diverse nature of feedstocks innately required for biomass conversion. As a result, a "cocktail" of almost 50 different cellulase enzymes must be used together in order to decompose appreciable amounts of cellulose.[7]

The second approach is through acid catalyzed hydrolysis. One drawbacks of acid catalyzed hydrolysis is a lack of control over selectivity leading to a hydrolysis to glucose, as well as uncontrolled side-reactions and other degradation products. Additionally, the corrosive conditions associated with an aqueous acid environment require corrosive resistant materials for reactors, which increases costs.[23]

Additionally, both methods of pretreatment require extensive pretreatment after reactions are completed, further increasing costs.[7] One option that has been proposed as a possible solution to this challenge is the use of solid acid catalysts. Solid acids theoretically combine the robust catalytic activity of liquid acids without the corrosive environment, and separations are simpler because of the different phases leading to a simple filtration. Solid acids are discussed in more detail in the next section.

[23] Xu, Zhaoyang, and Fang Huang. "Pretreatment Methods for Bioethanol Production." *Applied biochemistry and biotechnology* 174.1 (2014): 43–62. Web.

2.3 Solid Acid Catalysts

Solid acid catalysts have been under recent investigation for the aforementioned benefits. They can generally be grouped into four distinct categories; micro- and mesoporous materials, metal oxides, metal supported catalysts, and sulfonated polymers. Micro- and mesoporous materials (i.e. zeolites) have the additional of diffusion limitations, which is particularly difficult for cellulose hydrolysis because cellulose is insoluble. Some metal oxides can support both Lewis and Brønsted acid sites, but often require high catalyst loading and other undesirable conditions such as microwave irradiation. Metal supported catalysts are commonly used and have shown to be efficient for small molecule transformation, but show no signs for being catalytically active for cellulose hydrolysis.[24]

The last category of solid acid catalysts is sulfonated polymers. In particular, polystyrene based acid catalysts have been reported to have favorable catalytic activity. The Pan catalyst, a sulfonated chloromethyl)polystyrene (CMP) polymer, for example has been reported to have 93% conversion of cellulose to glucose.[25] It has been proposed that this catalyst works similar to a cellulose enzyme, with the chloride groups forming binding interactions with cellulose, and the sulfonic acid groups catalyzing the cleavage of the beta (1→4) glycosidic bond. Figure 4 below depicts such a mechanism.[13]

[24] Hara, Michikazu, Kiyotaka Nakajima, and Keigo Kamata. "Recent Progress in the Development of Solid Catalysts for Biomass Conversion into High Value-Added Chemicals." *Science and Technology of Advanced Materials* 16.3 (2015): 1–22. Web.

[25] Yang, Qiang, and Xuejun Pan. "Synthesis and Application of Bifunctional Porous Polymers Bearing Chloride and Sulfonic Acid as Cellulase-Mimetic Solid Acids for Cellulose Hydrolysis." *Bioenergy Research* 9.2 (2016): 578–586. Web.

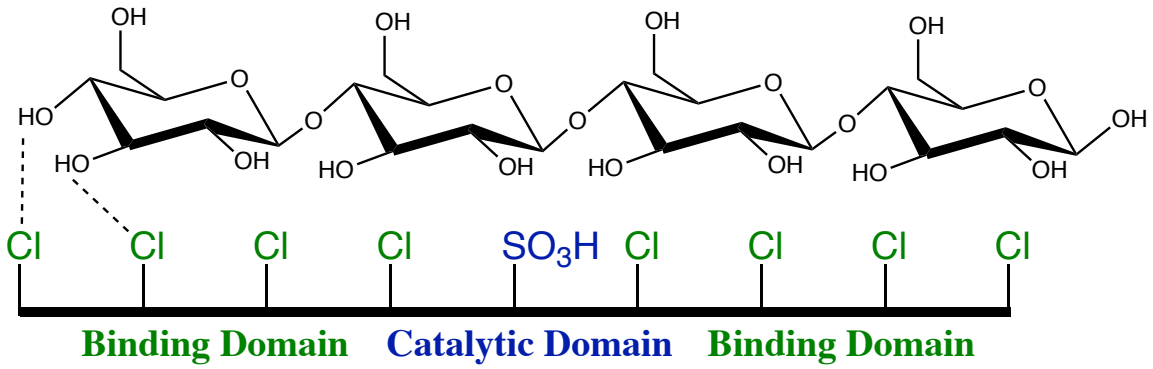

Figure 4: Proposed Mechanism of sulfonated CMP based solid acid catalysts.[26]

A serious mechanistic study into the catalytic mechanism for this catalyst and reaction however is lacking and would help lead to a better understanding of the kinetics f the reaction. With this understanding, rational catalyst design is possible and could leader to ore efficient catalysts.

2.4 Kinetic Modeling

Kinetic modeling is a powerful approach when looking at kinetic data. With a given mechanism, set of rate parameters, and reactor conditions it is possible to solve a system or ordinary differential equations to determine concentrations of given products and reactants in a reactor over time.

In heterogeneous catalysis (what would be expected of a solid acid catalyst) microkinetic modeling is often employed. Microkinetic modeling breaks down a reaction into a set of elementary reactions, such as a species adsorbing to a catalyst surface, a specific atom attaching or detaching, and a species releasing from the surface. Most of these steps are difficult to determine experimentally, and thus are often informed by computational methods such as density functional theory.[26]

General kinetic modeling is typically employed for reactions that occur homogenously (as expected via liquid acid catalysis). Under homogenous conditions, diffusion and mass-transfer limitations are often considered sufficiently

[26] "Microkinetic Modeling." Microkinetic Modeling | Schmidt Group, schmidt.chem.wisc.edu/microkinetic-modeling.

negligible with adequate mixing and thus the more macroscopic approach is often suitable.[27] Since the kinetics of cellulose hydrolysis have been well studied, the kinetic data and some modeling approaches are discussed in the following sections.

2.4.1 Acid Catalyzed Cellulose Hydrolysis

Acid catalyzed hydrolysis of cellulose is a well-studied topic that has been reviewed for more than 70 years. Despite significant attention, the topic is still difficult to address. Substrates vary widely in cellulosic structure and consequentially determining general kinetic parameters for the reaction is difficult, with little consensus in the literature. For example, SriBala et al. summarizes 9 different studies on the matter as summarized in Table 1. The parameters are given for the reaction of the decomposition of cellulose, which takes the Arrhenius form, and k_{10} is the pre-exponential factor, E_{a1} the activation energy, and m_1 the exponent applied to the acid concentration. Notably, all of these studies used H_2SO_4 as the acid and use the wt % of acid in the kinetic expression.

[27] Steinfeld, Jeffrey I., et al. Chemical Kinetics and Dynamics. Prentice Hall, 1999.

Substrate	Reaction Conditions	k_{10} (min^{-1})	E_{a1} (kJ/mol)	m_1
cellulose pulp from sugar cane bagasse	acid: 0.07–0.28 wt % temp: 180–230 °C	1.3×10^{19}	184.9	
douglas fir	acid: 0.4–1.0 wt % temp: 170–190 °C	1.73×10^{19}	179.5	1.34
microcrystaline cellulose	acid: 30–70 wt % temp: 25–40 °C	2.946×10^{10}	127.2	6
paper refuse	acid: 0.2–1.0 wt % temp: 180–240 °C	28×10^{19}	188.7	1.78
municipal solid waste	acid: 1.3–4.4 wt % temp: 200–240 °C	1.94×10^{16}	171.61	1
α-cellulose	acid: 0.2–1.0 wt % temp: 220–240 °C	1.2×10^{19}	177.6	1.3
solka-floc	acid: 0.5-2.0 wt % temp: 180–240 °C	1.22×10^{19}	177.8	1.16
filter paper	acid: 0.4–1.5 wt % temp: 200–240 °C	1.22×10^{19}	178.9	1.16
hardwood	acid: 4.41–12.2 wt % temp: 170–190 °C	1.66×10^{16}	165.34	1.64

Table 1: Overview of literature on acid catalyzed cellulose hydrolysis, adapted from SriBala et.al.[28]

Aside from the study done with microcrystalline cellulose, these studies all represent dilute-acid, high temperature reaction conditions. To compare these, it is helpful to look at the conversion if cellulose given each set of kinetic parameters at a given acid concentration and temperature. Figure XX below shows the results of cellulose conversion with an acid concentration of 0.5 wt% and a temperature of 175 °C.

[28] SriBala, G., and R. Vinu. "Unified Kinetic Model for Cellulose Deconstruction via Acid Hydrolysis." Industrial and Engineering Chemistry Research 53.21 (2014): 8714–8725. Web.

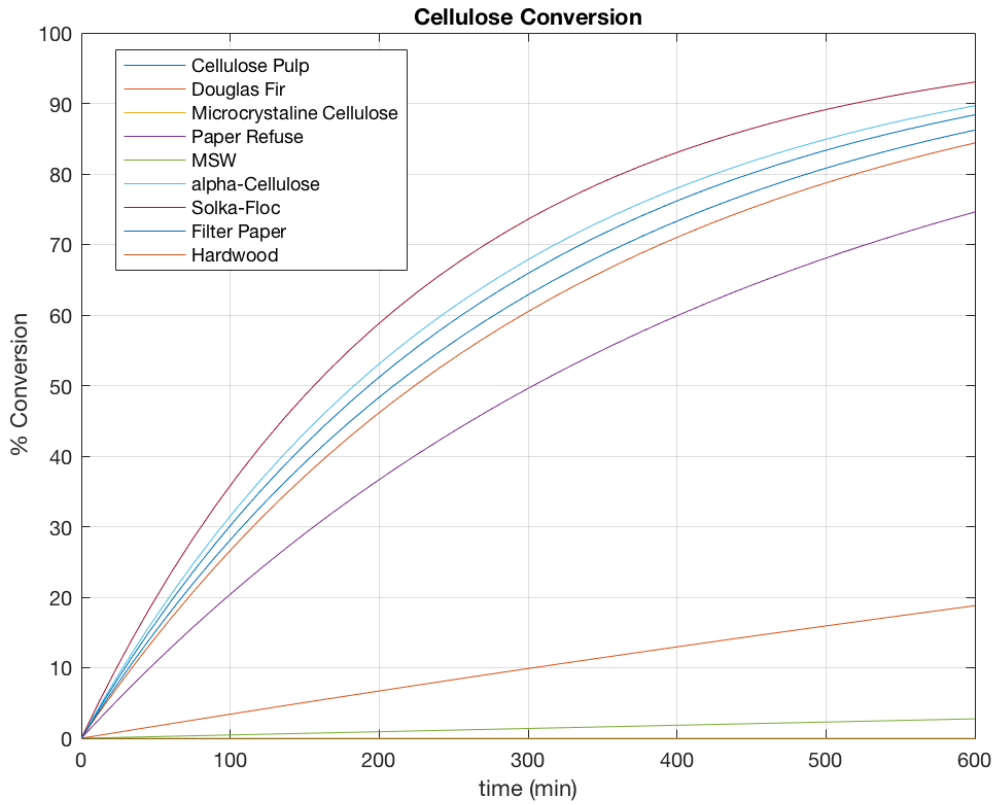

Figure 5: Conversion of cellulose with various rate parameters reported in the literature.

Clearly there is a discontinuity in rate parameters based on reaction conditions and substrate characteristics. As shown above in Figure 5 cellulose conversion over a 10-hour period at consistent conditions yields conversions ranging from 0% to 93% based on which kinetic parameters are used. Recent models have attempted to take into account the differences in substrates, and the non-homogeneity of the reaction, by incorporating factors such as the degree of polymerization and cellulose crystalinty, but a unified kinetic model is still to be found.[21,29]

[29] Yan, Lishi et al. "A Comprehensive Mechanistic Kinetic Model for Dilute Acid Hydrolysis of Switchgrass Cellulose to Glucose, 5-HMF and Levulinic Acid." *RSC Advances* 4.45 (2014): 23492. Web.

2.4.2 Acid Catalyzed Glucose Decomposition

Acid catalyzed reactions of glucose are an equally well studies set of reactions, with slightly more consensus due to the fact that all chemistry occurs in a homogenous liquid solution (all reactants are soluble). Despite this there are a number of different mechanisms that have been proposed for the decomposition of glucose to levulinic acid and other products.

Some mechanisms propose the reaction proceeds via a 5 membered ring (i.e. fructose) intermediate and then continues to hydroxymethylfurfural (HMF), but most consider this a non-limiting step disregard this intermediate.[30] It is well accepted that glucose and HMF degrade into non-soluble carbon based side-products referred to as humins. Lastly it is generally well accepted that the energy barrier to go from glucose to HMF is higher than for the decomposition/rehydration of HMF to levulinic and formic acid. As a result, HMF is quickly consumed as it is formed, and generally is not a major product under reaction conditions for cellulose hydrolysis.

Table 2, adapted from Weingarten et al. below provides a concise overview of literature available on aqueous acid catalyzed glucose reactions displaying both proposed mechanisms and kinetic parameters.[31]

[30] Garcés, Diego, Eva Díaz, and Salvador Ordóñez. "Aqueous Phase Conversion of Hexoses into 5-Hydroxymethylfurfural and Levulinic Acid in the Presence of Hydrochloric Acid: Mechanism and Kinetics." *Industrial and Engineering Chemistry Research* 56.18 (2017): 5221–5230. Web.

[31] Weingarten, Ronen et al. "Kinetics and Reaction Engineering of Levulinic Acid Production from Aqueous Glucose Solutions." *ChemSusChem* 5.7 (2012): 1280–1290. Web.

Proposed model[a]	Reaction conditions[b]	Ea[c] [kJ mol^{-1}]
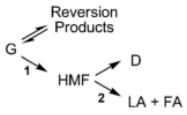	T = 100–150 °C [HCl] = 0.35 M $[G]_0$ = 1 wt%	Ea_1 = 133 Ea_2 = 95
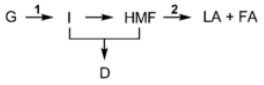	T = 140–250 °C $[H_2SO_4]$ = 0.0125–0.4 M $[G]_0$ = 5–17 wt% $[HMF]_0$ = 1–2 wt%	Ea_1 = 137 Ea_2 = 97
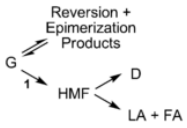	T = 180–224 °C $[H_2SO_4]$ = 0.05–0.4 M $[G]_0$ = 0.4–6 wt%	Ea_1 = 128
	T = 170–230 °C $[H_3PO_4]$: pH 1–4 $[G]_0$ = 0.6–6 wt% $[HMF]_0$ = 0.3 wt%	Ea_1 = 121 Ea_2 = 56
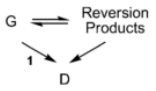	T = 200–230 °C $[H_2SO_4]$ = 0.005–0.02 M $[G]_0$ = 2 wt%	Ea_1 = 139
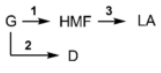	T = 170–190 °C $[H_2SO_4]$ = 0.1–0.5 M $[G]_0$ = 5 wt%	Ea_1 = 86 Ea_2 = 210 Ea_3 = 57
	T = 98–200 °C $[H_2SO_4]$ = 0.05–1 M $[G]_0$ = 2–15 wt% $[HMF]_0$ = 1–11 wt%	Ea_1 = 152 Ea_2 = 165 Ea_3 = 111 Ea_4 = 111
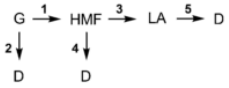	T = 180–280 °C non-catalyzed $[G]_0$ = 1 wt% $[HMF]_0$ = 0.75 wt% $[LA]_0$ = 0.5 wt%	Ea_1 = 108 Ea_2 = 136 Ea_3 = 89 Ea_4 = 109 Ea_5 = 31
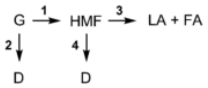	T = 140–180 °C 0 M < [HCl] ≤ 1.0 M $[G]_0$ = 2–20 wt% $[HMF]_0$ = 4–16 wt%	$Ea_1 = 160 \pm 5$ $Ea_2 = 51 \pm 2$ $Ea_3 = 95 \pm 6$ $Ea_4 = 142 \pm 26$

[a] G = glucose; HMF = 5-hydroxymethylfurfural; LA = levulinic acid; FA = formic acid; I = intermediate; D = decomposition products (humins). [b] Units of feedstock and acid concentrations were converted for consistency. Values were rounded to the nearest unit. [c] Activation energy.

Table 2: Overview of literature on acid catalyzed glucose decomposition, adapted from Weingarten et.al.[31]

2.5 Objective

It is apparent that the use of solid acid catalysts for biomass pretreatment and upgrading could drastically reduce costs for bioproducts, making them cost-competitive with petroleum based products with added sustainable benefits. One specific category of solid acid catalysts of interest are sulfonated (chloromethyl)polystyrene (CMP) based catalysts, deemed "cellulose mimetic" catalysts because they are thought to catalyze cellulose hydrolysis in a similar fashion to cellulose enzymes. The exact kinetic mechanism for catalysis is still unclear and if elucidated could lead to the rational design of more efficient catalysts. Two polystyrene based catalysts of interest (CMP and CMP-SO_3H-0.3) in particular are shown below in Figure 6.

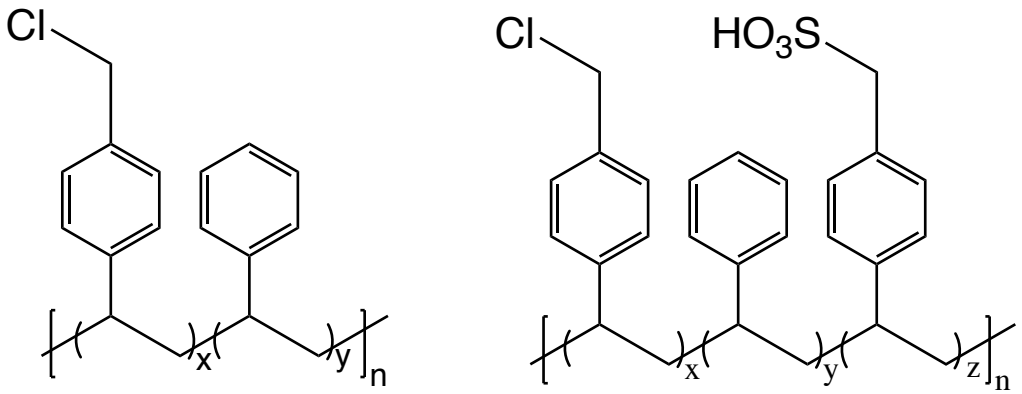

Table 6: (Chloromethyl)polystyrene based acid catalysts CMP (left) and a sulfonated derivative CMP-SO_3H-0.3 (right).

The purpose this work was to investigate the structural hydrothermal stability of these types of solid acid catalysts in an attempt to elucidate structural features that may be responsible for catalytic activity. Macro-kinetic modeling was employed to determine if catalytic effects could be attributed solely to the leaching of liquid acid from the solid acid catalyst, or whether the solid acid had additional catalytic activity.

Chapter 3: Methodology

This project combined both experimental and computational methods to investigate polystyrene based solid acid catalysts. Experimentally, methods were developed to explore the thermostability of catalysts under reaction conditions. Computationally, macro-scale molecular modeling was used to model the progress of the reaction of cellulose hydrolysis. Ultimately, experimental data was used to inform the computational kinetic model and gain insights into the mechanism of catalysis by these materials for cellulose hydrolysis.

3.1 Catalyst Synthesis

CMP is a commercially available product. For this study CMP was obtained from Millipore Sigma (Burlington, MA) with ~5.5 mmol/g of Cl and a particle size of 16-50 mesh. The sulfonated CMP derivatives were synthesized in the following manner based on a procedure adapted from Zuo et al. and Tyufekchiev et al.[32,33]

This project focused on the synthesis of a partially sulfonated CMP derivative where only some of the chloride functional groups have been exchanged with sulfonic acid groups. This derivative, CMP-SO_3H-0.3, utilized 0.3 equivalents of reagents to ensure that not all chloride functional groups are converted. Other variations on this synthesis are possible, including a higher ratio of sulfonic acid to chloride groups as well as total exchange for sulfonic acid groups. Figure 7 below outlines the polymer modification process and necessary steps, with explicit details included below.

[32] Zuo, Yong, Ying Zhang, and Yao Fu. "Catalytic Conversion of Cellulose into Levulinic Acid by a Sulfonated Chloromethyl Polystyrene Solid Acid Catalyst." *ChemCatChem* 6.3 (2014): 753–57.Web.

[33] Tyufekchiev, Maksim et al. "Cellulase-Inspired Solid Acids for Cellulose Hydrolysis: Structural Explanations for High Catalytic Activity." *ACS Catalysis* 8.2 (2018): 1464–1468. Web.

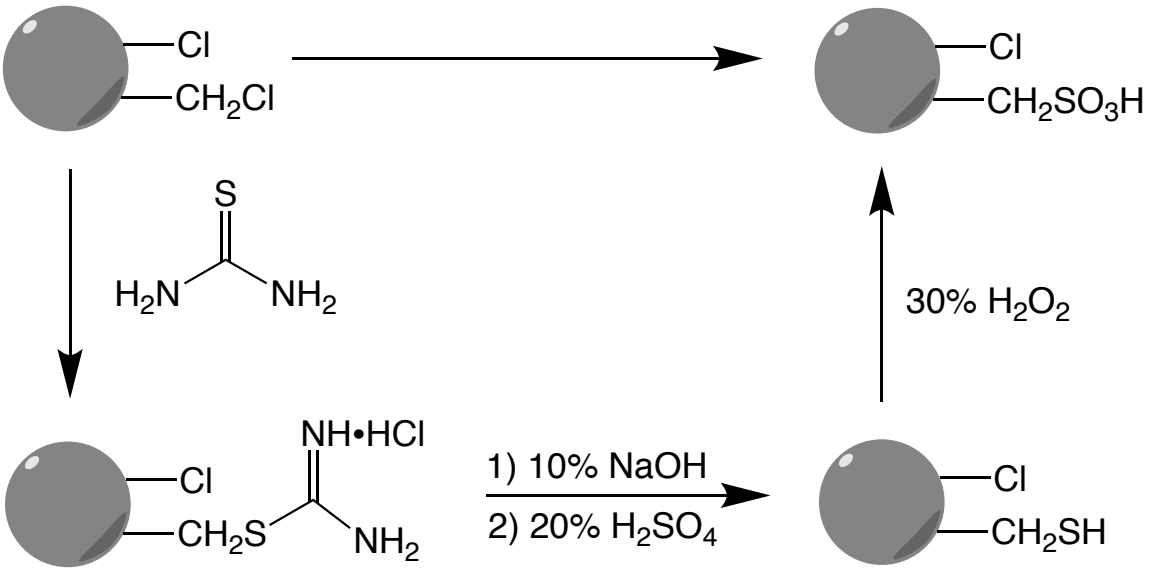

Figure 7: Synthesis steps for polymer modification to produce sulfonated CMP derivatives.[33]

First, 12g of CMP beads (~66 mmol of Cl, 1.00 equivalent) were combined with 120 mL of dimethylformamide(DMF) in a 250 mL round-bottom flask. The mixture was capped with a rubber septum and heated in an oil bath at 120°C for 4 hours with a constant stir rate (individual stir bars in both the round-bottom flask and oil bath) at a rate of 150 rpm. The beads were then filtered via vacuum filtration and washed with 150 mL of methanol.

Next a thiourea solution was made by dissolving 1.5 g of thiourea (20mmol, 0.30 equivalents) in 120 mL of methanol. The undried beads were combined with the thiourea solution and heated in a round-bottom flask capped with a rubber septum. The reaction took place at 65°C for 1 hour and 15 minutes. Afterwards, the polymer beads were isolated via vacuum filtration and washed with 500 mL of DI water.

After filtration, the polymer beads were reacted with 120 mL of 1M NaOH (120 mmol, 1.80 equivalents) in a round-bottom flask capped with a rubber septum at 100°C for 45 minutes. The beads were isolated via vacuum filtration and washed with 2000 mL of DI water. The washed beads were then reacted with 180 mL of 1M H_2SO_4 for 5 hours at 40°C. Finally the beads were isolated via vacuum filtration and

washed excessively with DI water, until the resulting filtrate registered a pH of 6 or higher. The polymer beads were then dried in a 65°C oven overnight.

3.3 Catalyst Characterization

Catalyst characterization was necessary for both confirming successful synthesis of the sulfonated CMP derivatives, as well as determining any structural changes to the catalyst after being exposed to reaction-like condition. The characterization techniques used in this work include both Raman and Infrared (IR) Spectroscopy. By using both of these techniques, the presence of specific functional groups (-Cl, -SO_3H,-OH) on the catalyst surface could be identified.

3.3.1 Infrared Spectroscopy

Infrared spectroscopy (IR) is a common analytical tool that can help in the identification of chemical functional groups. Specifically for this work, functional groups including hydroxyl (-OH), chloride (-Cl), and sulfonic acid (-SO_3H) groups were of particular interest. IR spectroscopy exposes samples to a range of infrared light, and detects which wavelengths of light are absorbed by the sample. Chemical species (i.e. functional groups) absorb specific wavelengths of light, which causes vibrations within the bonds of the molecule, and are specific to the individual functional groups because these are resonance frequencies.[34] As a result, the innate polarizability (dipole moment) of specific bonds leads to different resonant frequencies, and consequentially specific wavelengths of absorption.

IR analysis was completed using a Vertex 70 Bruker FT-IR with a Specac Golden Gate ATR accessory. Initially, 1024 background scans were performed to calibrate the instrument and reduce any potential noise. Sample beads were spread on the Golden Gate ATR accessory platform, and the clamp was closed on multiple beads, effectively crushing them. As a result, IR spectroscopic results detailed

[34] Lambert, Joseph B. *Organic Structural Spectroscopy*. Upper Saddle River, NJ: Prentice Hall, 1998. Print.

information about the bulk properties of the catalyst species. The sample was subjected to 1024 scans and the data was processed using Opus software.

3.3.2 Raman Spectroscopy

Raman spectroscopy probes molecules by exposing the sample to a monochromatic light source and measuring the resulting scattering produced by the molecule. Different molecules have specific Raman molecular fingerprints based upon the polarizability of the molecules electrons. One major advantage of Raman spectroscopy is that it only weakly detects the presence of hydroxyl function groups, because while hydroxyl functional groups have an innately strong dipole, the polarizability of this bond is weak because of the naturally strong dipole.[3] The lack of detection of hydroxyl groups is actually a positive feature of Raman, because it allows for greater visibility of other "fingerprint regions" that allow for identification of other functional groups, specifically chloride and sulfonic acid groups in this particular case of interest.

Raman analysis was completed using a Horiba XploRa Raman Microscope. The system was calibrated using a silicon chip prior to sampling. Sampling conditions included an objective lens of 100x zoom, a grating of 600, a 100% filter with a monochromatic light source of 785 nm at 100 mW, a slit of 100 and a hole of 300. Each sample had a 3 second acquisition time with data averaged over 100 scans. Due to the porous nature of the catalyst surface, the laser was often scattered, but the laser was still able to be focused within a 5-10 μm dot. A sample focused laser point is shown in Figure 8 below.

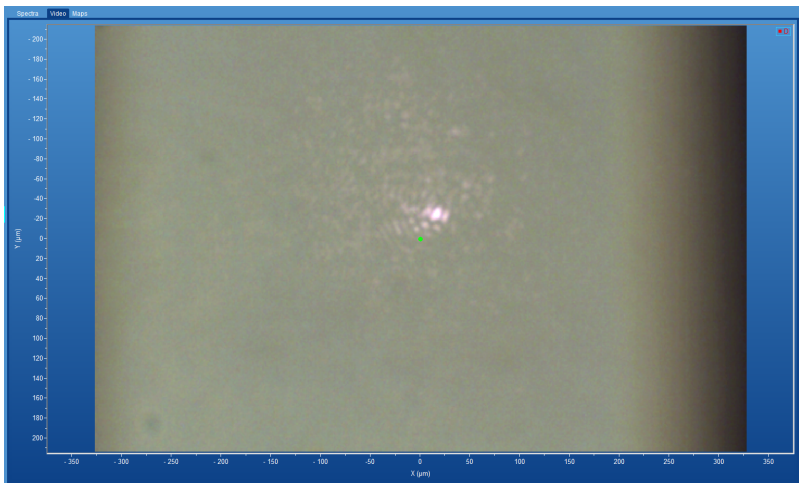

Figure 8: Raman laser (pink) focused on surface of catalyst bead.

Data was processed using LabSpec 6 software where a baseline correction was necessary. The baseline was corrected using a 4-6 degree polynomial with ~50 points. Lastly for comparison between spectra, all spectra were normalized using the 1610 cm^{-1} peak, corresponding to the aromatic species. This peak was used for normalization because all catalyst species were made of a bulk polystyrene polymer that was constant for all catalysts, and thus did not change between different samples.

3.4 Catalyst Stability Experiments

In order to determine the thermal stability of catalyst species, a time study was performed under reaction like conditions. 0.2 g of catalyst and 2 mL of 17.8 MΩ ultrapure water were added to a 15mL heavy wall pressure vessel, acquired from Chemglass Life Sciences LLC (Vineland, NJ), which served as a closed batch reactor. A stir bar was added to the reactor, which was then capped and sealed. A hot oil bath was used for heating with a set point of 175°C and a stir rate of 200 rpm. Experiments were carried out in triplicate, and the reactors were set in the oil bath as shown below in Figure 9.

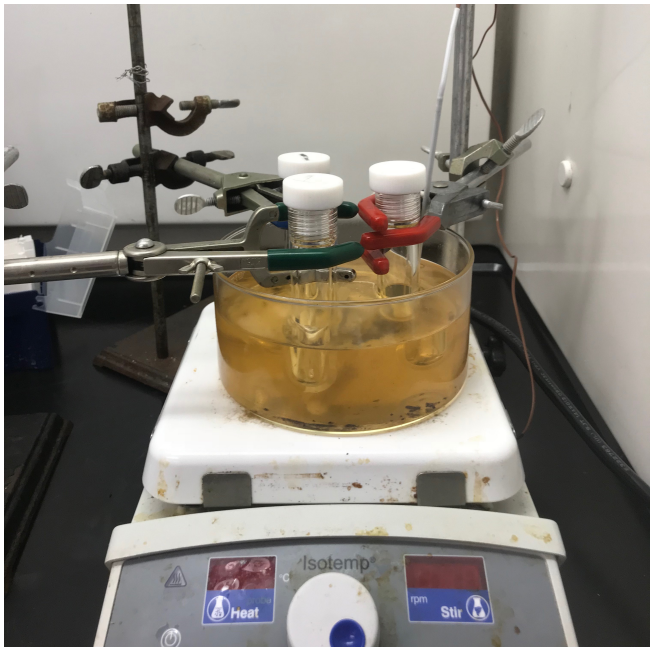

Figure 9: Placement of reactor vials within hot oil bath.

Experiments were carried out for various reaction times, including 30 minutes, 1 hour, 2 hours, 4 hours, 6 hours, 8 hours, and 10 hours. After the allotted reaction time, the reactors were immediately removed from the oil bath and quenched using cooling water. The reactors were then allowed to equilibrate to room temperature.

To obtain data on hydrogen ion concentration of the resulting reactor contents, the pH of the liquid reactor contents was measured using a VWR Scientific model 8000 pH meter. Prior to measuring the pH of the liquid reactor contents, the pH meter was calibrated using pH buffer solutions of pH 4 and pH 7, acquired from Micro Essential (Brooklyn, NY). The liquid contents were then collected using a 3 mL Luer Lock syringe with a 27G needle to ensure that no solid particulates were collected along with the liquids. The remaining solid catalysts particles were collected and allowed to dry at room temperature before further characterization using IR and Raman spectroscopy, as described above.

The liquid contents were further analyzed using Ion Chromatography (IC). IC separates ions based upon the different ions affinity to an ion exchanger. Once separated from each other, the ions elute through the system and are detected

based on the conductivity of the resulting solution (ions serve as charge carriers and therefore increase the conductivity of a solution). For these experiments, IC analysis was performed using a Dionex ICS-2100 instrument equipped with a IonPac AG15 2x50 mm guard column and a IonPac AS15 2x50 mm column at 30°C. A DS6 Conductivity cell was used as the detector. The injection volume was 100uL, and the eluent was 38 mM KOH with a flow rate of 0.25 mL/min. For calibration, a calibration curve was generated using an ion standard that ranged from 0.5ppm to 10ppm.

3.5 Investigation of the Experimental Apparatus

The kinetics of this reaction is highly sensitive to temperature, and therefore it is important that the temperature control of the system is precise. The experimental apparatus consisted of a silicone oil bath on a Fischer Scientific Isotemp hotplate. With the understanding that there could be non-uniformities of the temperature within the oil bath, experiments were designed to test what the temperature gradient might be.

A Teflon cap, fit for the glass reactor vial, was drilled through the top to allow a thermocouple to be inserted. The thermocouple was fit tight with a metal ferrule and screw wrapped with Teflon tape to ensure an airtight seal. The end of the thermocouple was set so that it was slightly above the bottom of the glass reactor tube. A picture of the assembled measurement apparatus is shown below in Figure 10.

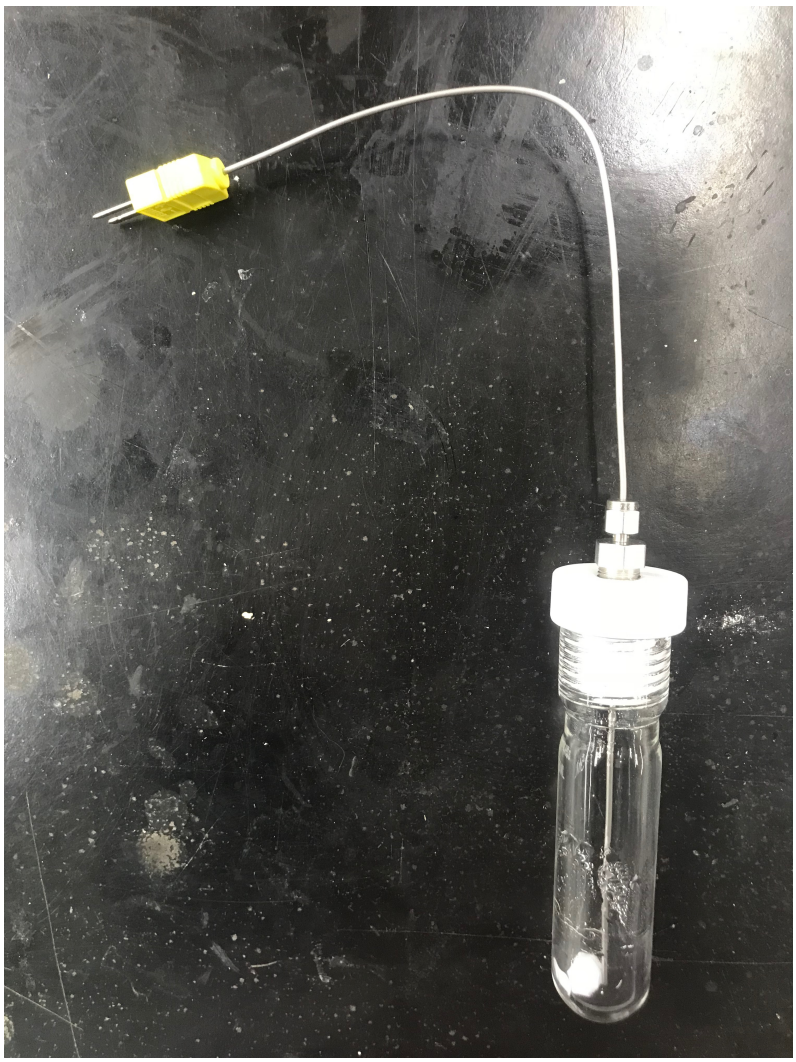

Figure 10: Assembled apparatus for measuring temperature within reactors.

To investigate the heating of the experimental apparatus the oil bath was set to a temperature of 175°C and a stir rate of 200 rpm as in all other experiments. The system was allowed to equilibrate, and 2 mL of DI water was added to the reactor vial and the thermocouple and top screwed into place. The reactor vial was then placed into the oil bath as it would be for a standard experimental reaction, allowed to equilibrate after a few moments, and the temperature was recorded. The goal of this experimental portion was to map the temperature that exists within the liquid of the reactor dependent on its spatial orientation within the oil bath, and verify if there is any temperature range that exists. Accordingly, multiple radial positions and vial depths were tested, as shown in Figure 11 below.

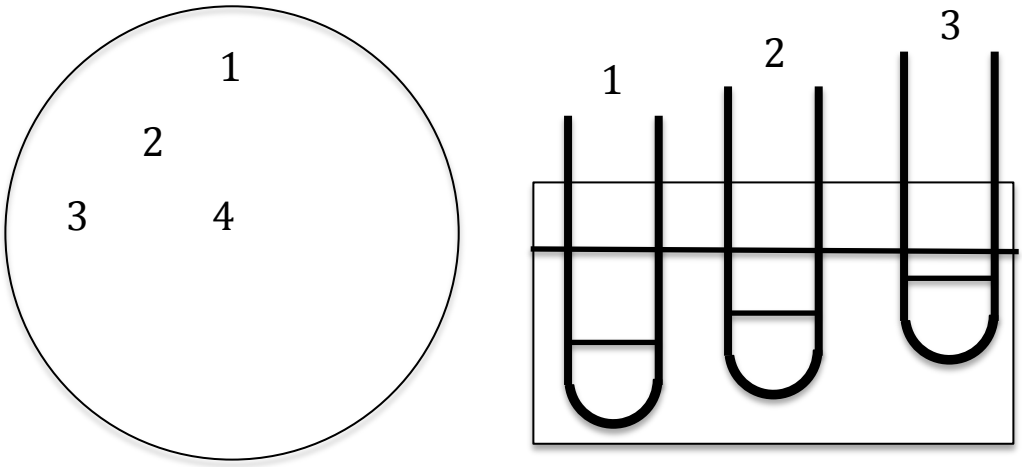

Figure 11: Various positions (radial on left, height depths on right) used for testing temperature variations within the oil bath.

3.6 Kinetic Modeling

Macro-kinetic modeling consisted of solving systems of differential equations. For this purpose MATLAB software was used, and kinetic rate parameters were taken from literature. The following sections detail how rate parameters were chosen from literature, the approach taken to set up and model the system in MATLAB, and how using experimental data a Monte Carlo approach was taken to describe experimental uncertainties within the model.

3.6.1 Choosing Kinetic Parameters

As shown in section 2.4, there is extensive literature regarding the reactions of liquid acid catalyzed cellulose hydrolysis and the associated by-products and side reactions. A kinetic model using kinetic parameters from a liquid acid mechanism would help to create a benchmark for what we would expect from the solid acid catalyst, if it were leaching liquid acid. By developing this model and comparing our data with the solid acid catalysts to that of the kinetic model, it is possible to see whether the solid acid is having any extra catalytic effects, or is simply leaching liquid acid, which is actually responsible for catalyzing the reaction.

Choosing which kinetic parameters and which studies to rely on became an important facet of this work. Ultimately, the results from studies that had similar reaction conditions were used for the kinetic modeling.

For the rate constant for the acid catalyzed hydrolysis of cellulose, Saeman's results from *Kinetics of Wood Saccharification - Hydrolysis of Cellulose and Decomposition of Sugars in Dilute Acid at High Temperature* published in 1945 were used.[35] This is one of the first works on the subject, and was performed in the temperature range of 170°C-190°C with an acid concentration of 0.4-1.0 wt% H_2SO_4. While the acid used, H_2SO_4, is not the exact liquid acid expected to be leaching from CMP based solid acid catalysts (it is likely HCl), both are strong mineral acids and are expected to have similar effects. Additionally, the substrate used, douglas fir, differs from the substrate in this study, microcrystalline cellulose, (MCC), but sufficient literature on MCC hydrolysis was not found. Lastly, Saeman's work is highly regarded in the field and continues to be cited, giving merit to his findings, which are still relevant and continue to be used today.

The kinetic rate constant given by Saeman takes the form found below in equation 1 where $A_{x,o}$ is a pre-exponential factor, A is the acid concentration in wt% of H_2SO_4, n is an exponent to scale the reaction dependence on acid concentration, E_a is the activation energy, R is the universal gas constant and T is temperature in Kelvin.

$$k_x = A_{x,o} * A^n * \exp\left(\frac{-E_{a,x}}{2.303 * R * T}\right)$$

Equation 1: Kinetic rate constant given in Saeman's form.[17]

For the kinetic parameters for the homogenous reaction of glucose to levulinic acid, namely the reactions involving glucose dehydration to hydroxymethylfurfural (HMF) and the rehydration of HMF to from levulinic acid and

[35] Saeman, Jerome F. "Kinetics of Wood Saccharification - Hydrolysis of Cellulose and Decomposition of Sugars in Dilute Acid at High Temperature." *Industrial & Engineering Chemistry* 37.1 (1945): 43–52. Web.

formic acid, the kinetic parameters were taken from Weingarten et al.[31] The mechanism proposed by this study is shown below in Figure 12 and includes glucose to HMF, HMF to levulinic acid and formic acid, and the decomposition of both glucose and HMF to insoluble byproducts called humins.

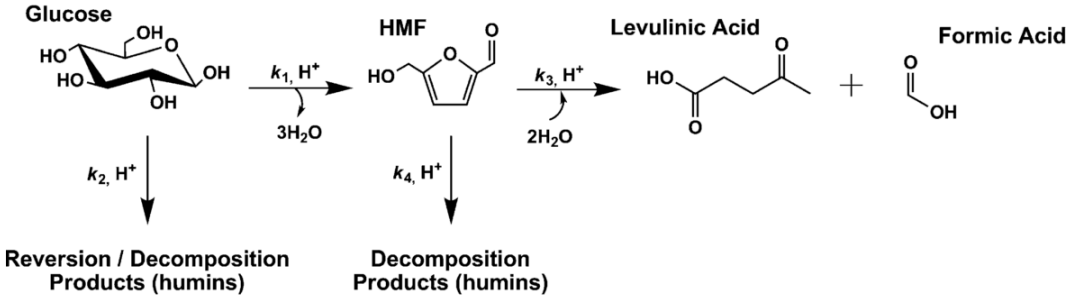

Figure 12: Reaction mechanism proposed by Weingarten et al.[31]

Weingarten's study was performed in the temperature range of 140°C-180°C with an acid concentration of 0-1.0 M HCl, both suitable for the modeling this work. While other kinetic studies have been performed regarding this mechanism, Weingarten has a mature treatment of the subject by explicitly studying the kinetic parameters of each individual reaction, not the mechanism as a whole. Additionally, the activation energies are consistent with the rest of literature findings.

The kinetic rate constants given by Weingarten et al. take the form found below in equations 2 and 2. Equation 1 describes how the pre-exponential factor, A_x, is dependent on the acid concentration. Equation 2 shows that the kinetic rate constants follow the standard Arrhenius model.

$$A_x = A_{x,o} * \left(H_{x,o} + [H^+]^{n_x}\right)$$

Equation 1: Pre-exponential factor dependence on acid concentration, given by Weingarten et al.[31]

$$k_x = A_x * \exp\left(\frac{-E_{a,x}}{R * T}\right)$$

Equation 2: Kinetic rate constant given in Arrhenius form.

3.6.2 General Modeling Approach

The mechanism used in this study combines the kinetic parameter of Saeman to from cellulose to glucose with those given for the homogenous reactions involving glucose to levulinic acid given by Weingarten et al.[17,18] The mechanism is shown in Figure 13 and the exact kinetic parameters are given in Table 3 below.

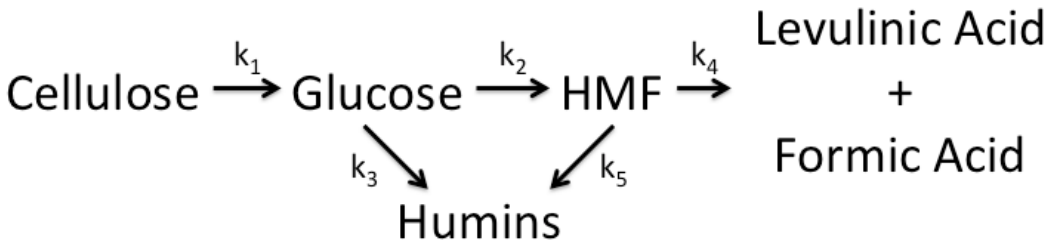

Figure 13: Reaction mechanism proposed by combining the results of Saeman and Weingarten et al.

x	$A_{x,o}$	Ea_x	$H_{x,o}$	n_x
1	1.73E+19	179.5	n/a	1.34
2	2.75E+18	160.16	0	1.290
3	7.24E+03	50.68	0.29	2.764
4	3.16E+11	94.72	0	1.176
5	6.76E+16	141.94	0	1.176

Table 3: Kinetic rate parameters used for kinetic modeling.[17,18]

Differential rate laws can be applied to each species in the reaction mechanism to create a system of ordinary differential 1s with respect to time. By solving for these differential equations simultaneously it is possible to predict the concentration of any given species at any time. The system of differential equations used to describe the system can be found below in Equations 3-6. Each species represented using abbreviations: C is for cellulose, G is for glucose, HMF is for

hydroxymethylfurfural, and LA is for levulinic acid. In addition to these differential equation and explicit kinetic parameters, the model captured the leaching of liquid acid by defining the acid concentration as an explicit function of time.

$$\frac{d[C]}{dt} = -k_1 * [C]$$
$$\frac{d[G]}{dt} = k_1 * [C] - k_2 * [G] - k_3 * [G]$$
$$\frac{d[HMF]}{dt} = k_2 * [G] - k_4 * [HMF] - k_5 * [HMF]$$
$$\frac{d[LA]}{dt} = k_4 * [HMF]$$

Equations 3-6: Differential equations used to describe the reaction system.

MATLAB was used to solve the system of differential equations. Specifically, the *ode45* package was used, which is a typical numerical method for solving nonstiff systems of ordinary differential and employs a combined fourth and fifth order Runge-Kutta method.[36] The specific MATLAB code can be found in Appendix A.

3.6.3 Monte Carlo Methods

In order to take into account the variability of certain parameters within the model, a Monte Carlo method was employed. The kinetic model is particularly sensitive to the liquid acid concentration and temperature, and these two variables have the most variability experimentally. In order to account for this, both the temperature and the acid concentration were defined as an array of variables rather than explicit variables. For the acid concentration (a function of time), the pre-exponential factor was varied within a given range and temperature was explicitly

[36] "ode45." Solve Nonstiff Differential Equations - Medium Order Method - MATLAB ode45, www.mathworks.com/help/matlab/ref/ode45.html.

varied. Both variables were given a random distribution with the given range between an upper and lower bound.

Each variable was assigned 25 random values within the given range. This number produced a wide array of results that covered almost all possible scenarios while not exhausting significant computational resources. Each variable was looped over each other, resulting in a matrix of values that included each of the 25 possible acid concentrations paired with each of the 25 possible temperatures. In total, 625 simulations were run. The specific MATLAB code can be found in Appendix A.

Chapter 4: Results and Discussion

4.1 Experimental Results

While CMP is directly available as a commercial product, the sulfonated derivates were synthesized. After successful synthesis, the thermostability experiments were running, yielding interesting results that confirmed the leaching of chloride anions. Ultimately, dude to non-functioning equipment, the exact temperature variability experiments could not be run to completion.

4.1.1 Catalyst Synthesis

Successful catalyst synthesis of a partially sulfonated CMP derivative (CMP-SO_3H-0.3) was proven successful through catalyst characterization using Raman spectroscopy. Raman spectra of the surface of the polymer beads show significant decreases in the intensity of signature chloride stretches and the appearance of new signals that fall within the range of sulfonic acid peaks. Figure 14 below shows a Raman spectra of regular CMP and the sulfonated CMP-SO_3H-0.3 derivative that was synthesized for this work.

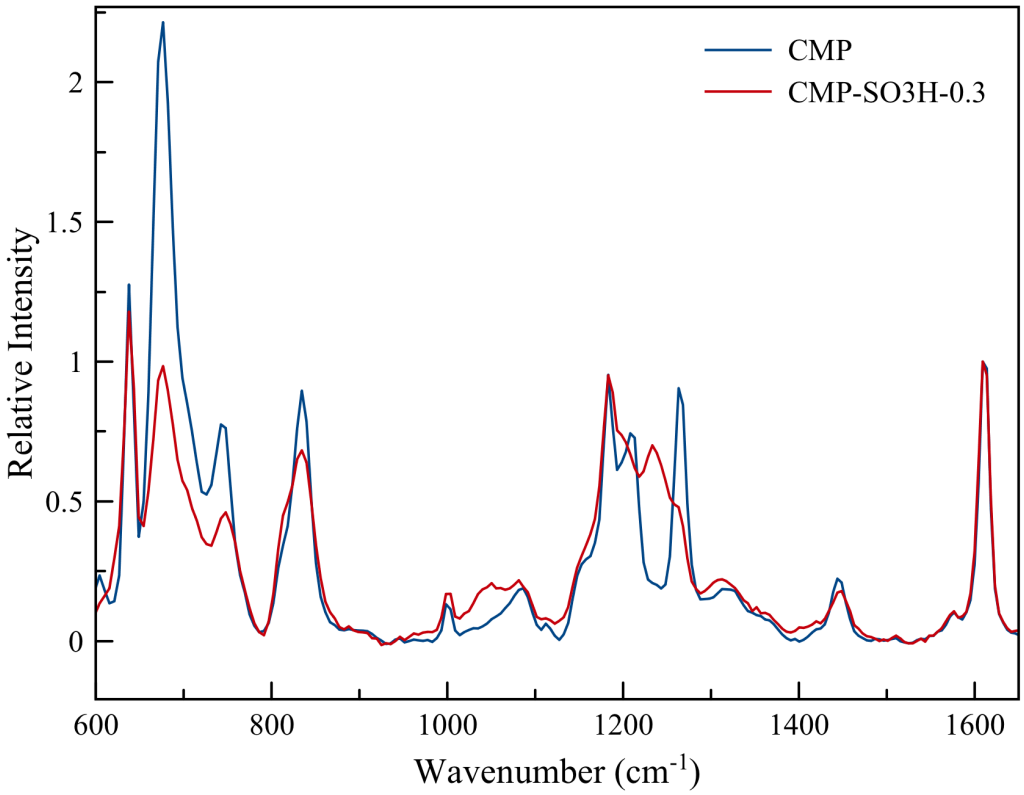

Figure 14: Raman spectra of surface of catalyst bead of CMP (blue) verse the synthesized CMP-SO_3H-0.3 (red).

The signature chloride peaks (-CH_2Cl) in the region of 650-750 cm^{-1} and at 1265 cm^{-1} have clearly decreased showing stripping of chloride from the surface of the catalyst. Additionally, new peaks specifically at ~1225 cm^{-1} evidence the attachment of sulfonic acid groups to the surface of the catalyst and therefore successful synthesis. It is important to note that while the chloride peaks have decreased in intensity, they have not entirely disappeared, indicating the presence of both functional groups on the surface of the catalyst as anticipated.

An attempt to synthesize a fully sulfonated derivative, CMP-SO_3H-1.2, proved unsuccessful. Significant chloride groups remained present on the surface. Difficulties during synthesis likely prevented its success, as the hot-plate used for maintaining temperature was likely not working properly at the time.

4.1.2 Thermostability of Catalysts

Hydrothermal stability experiments led to the conclusion that both catalysts, CMP and CMP-SO_3H-0.3, leached chloride anions into the aqueous reaction media. This was confirmed using both catalyst characterization as well as analysis of the reaction media.

Raman spectra of the catalyst beads taken at different time points show the disappearance of chloride again, this time however it is due purely to exposure to reaction conditions as opposed to synthetic manipulations. Figure 15 below shows a Raman spectra of CMP-SO_3H-0.3 immediately after synthesis, and then after being subjected to reaction conditions for ten hours.

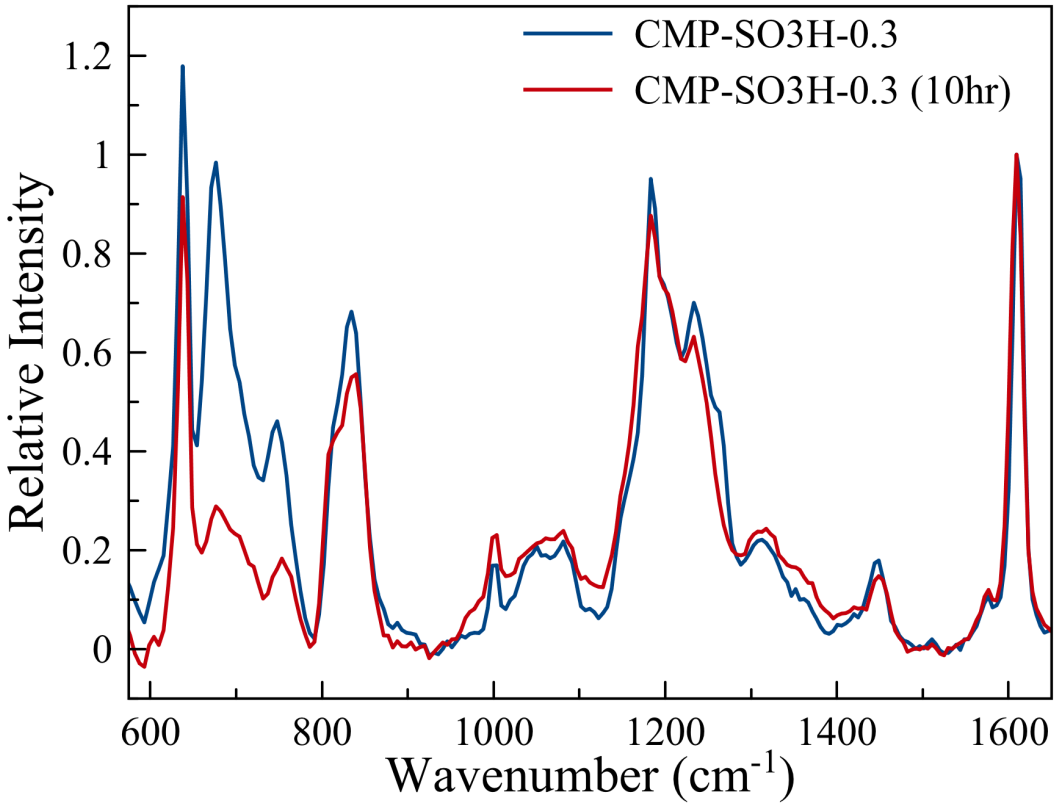

Figure 15: Raman spectra of surface of catalyst bead of CMP-SO_3H-0.3 after synthesis (blue) verse after being exposed to reaction conditions for 10 hours (red).

Again, the signature chloride peaks in the region of 650-750 cm^{-1} and at 1265 cm^{-1} have clearly decreased showing stripping of chloride from the surface of the catalyst. Notably, no new peaks have arisen, evidencing the fact that the chloride groups were likely hydrolyzed off and replaced by hydroxyl (-OH) groups. Due to the nature of Raman spectroscopy, these groups are not innately Raman active and thus would not result in any new peaks. Catalyst characterization proves the leaching of chloride groups, but analysis of the reaction media can give more quantitative information about how much and at what rate these groups are leaching.

Through pH measurements and analysis using IC, the concentration of [H^+], [Cl^-], and [SO_4^{-2}] were profiled for both CMP and CMP-SO_3H-0.3 over the course of 10 hours. Figure 16 and Figure 17 below show the aforementioned profiles, with an added first order fit to the acid concentration for CMP and CMP-SO_3H-0.3, respectively.

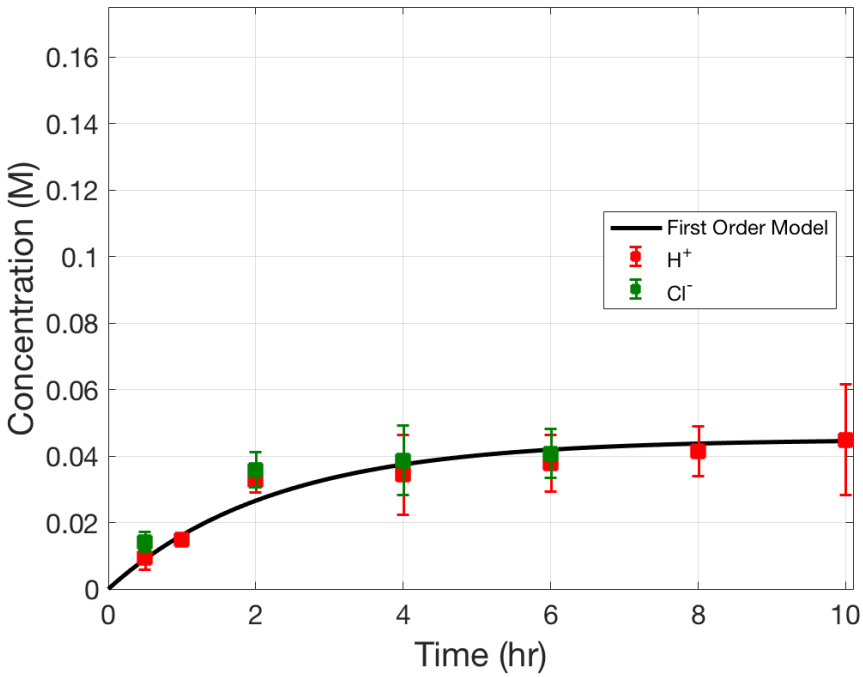

Figure 16: Analysis of liquid reaction media showing [H^+] and [Cl^-] concentrations over time for CMP.

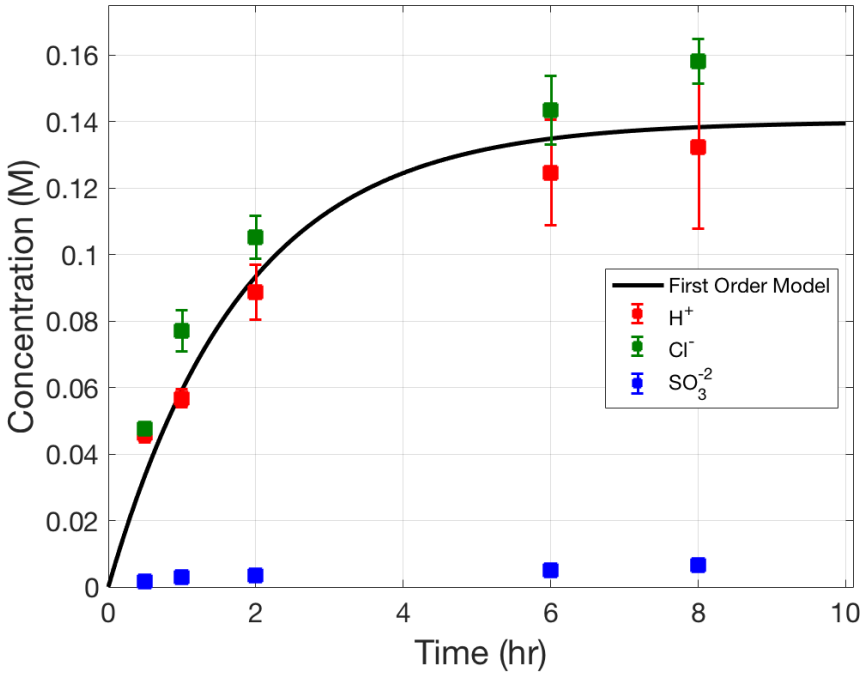

Figure 17: Analysis of liquid reaction media showing [H^+], [Cl^-] and [SO_4^{-2}] concentrations over time for CMP-SO_3H-0.3.

The close alignment, essentially a 1 to 1 ratio, between the concentrations of chloride and hydrogen ions again indicates hydrolysis of chloride groups from the catalyst bead. Additionally, it is noteworthy that for CMP-SO_3H-0.3, there were essentially no sulfate anions in the liquid reaction media, indicating that while chloride groups have the potential to hydrolyze and leach into the liquid media, sulfonic acid groups appear to be well attached to the catalyst bead and are resistant to hydrolysis. This finding is summarized in Figure 18 below.

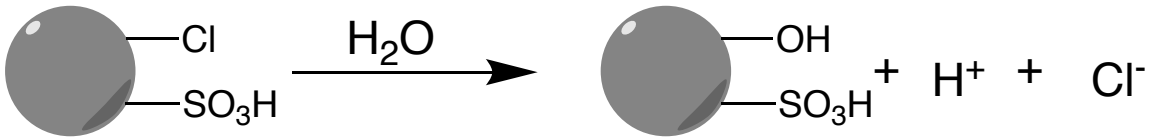

Figure 18: Hydrolysis of chloride groups from CMP based catalysts.

Another interesting observation is that while there are more chloride groups available for hydrolysis in CMP, the CMP-SO_3H-0.3 actually results in a higher liquid

acid concentration. This can be explained by the nature of the catalyst beads themselves. The CMP catalyst beads are extremely hydrophobic, while the CMP-SO_3H-0.3 beads are hydrophilic. Consequentially, within the reactor vial the CMP beads often float atop the aqueous reaction media and can even get stuck on the walls of the vial resulting in minimum interactions between the beads and the aqueous phase. The hydrophilic CMP-SO_3H-0.3 beads on the other hand are well mixed within the aqueous media and the surfaces of the beads are constantly in contact with liquid. Ultimately, this greater contact leads to more possibilities for chloride leaching.

Finally, a first order model was fit the match the trend of the experimental data for the [H^+] concentration, shown in Figures 16 and 17 as the solid black line. This resulted in the concentration for [H^+] as a function of time for each catalyst. This function was then incorporated into the kinetic model, to investigate the modes of catalysis. The model equations for both CMP and CMP-SO_3H-0.3 are given below in equations 7 and 8 respectively.

$$[H^+_{CMP}](t_{min}) = 0.045 \pm 0.015 * (1 - \exp(0.007435 * t_{min}))$$

Equation 7: Time dependent acid concentration determined experimentally for CMP, with time in minutes.

$$[H^+_{\mathrm{CMP-SO3H-0.3}}](t_{min}) = 0.135 \pm 0.025 * (1 - \exp(0.00708333 * t_{min}))$$

Equation 8: Time dependent acid concentration determined experimentally for CMP-SO_3H-0.3, with time in minutes.

4.1.3 Temperature Variations within Experimental Apparatus

By the time the apparatus to study the temperature variations of the reactor contents based on placement within the oil bath was assembled, the heat controller on the oil bath was unfortunately out of order. As a result, the temperature was anticipated to range anywhere from 167°C to 175°C (the set point). This temperature range, was made intentionally broad to capture as many possibilities

and as much uncertainty as possible based on some random sampling and preliminary experiments.

4.2 Modeling Results

The novel method used in this work, not previously employed in other modeling treatments of the subject, is the use of an acid concentration as a function of time. Typically the acid concentration is a fixed and controlled variable. In this study, it was important to capture the nature of the acid concentration, which increased over time based upon leaching from the solid acid catalyst. In order to do this, the time dependent liquid acid concentration, determined experimentally, was incorporated into the kinetic model and the governing differential equations.

4.2.1 Kinetic Modeling Aligns with Experimental Data

Actual cellulose hydrolysis data had been previously collected for both catalysts at 10 hours. This was compared with the kinetic modeling data to determine if the mechanism was predominated by the liquid acid catalyzed mechanism or if there were additional catalytic effects from the solid acid catalysts. To perform the Monte Carlo modeling, the temperature was varied from 167°C to 175°C as assumed before. The acid concentration was an exponential function of time with a pre-exponential factor that determined the final acid concentration, and was varied within the range indicated in equations 7 and 8 for CMP and CMP-SO_3H-0.3, respectively. The results of the Monte Carlo kinetic modeling with the experimental data plotted for both CMP and CMP-SO_3H-0.3 are shown in Figures 19 and 20 below.

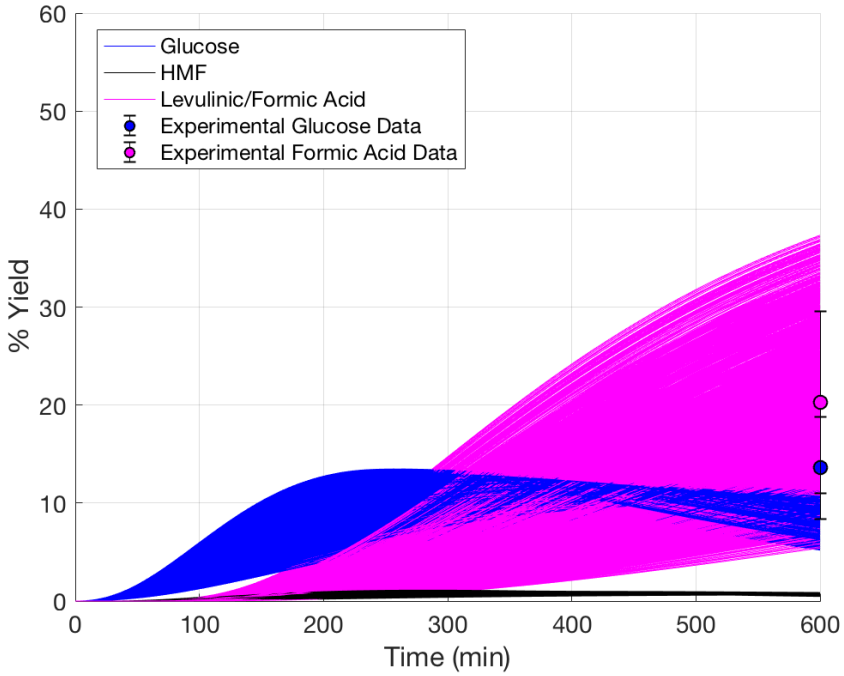

Figure 19: Kinetic modeling results with experimental cellulose hydrolysis data for CMP.

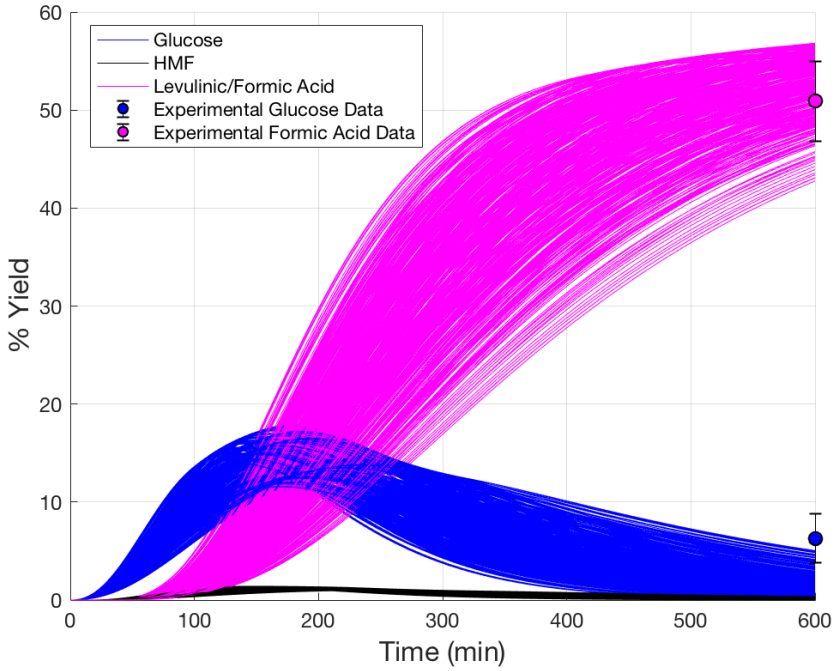

Figure 20: Kinetic modeling results with experimental cellulose hydrolysis data for CMP-SO_3H-0.3.

For both sets of kinetic models (CMP and CMP-SO_3H-0.3), the experimental data has good agreement for both glucose and formic acid yields. It is noticeable that even the standard deviation aligns with what is predicted by the Monte Carlo modeling which incorporates the experimental uncertainty into the kinetic model. The experimental glucose data is slightly above what is predicted, but perhaps the use of different kinetic parameters could perhaps alter these results.

The experimental data aligning with the liquid acid catalyzed kinetic model. This points towards the fact that the reaction is likely being catalyzed by a homogenous acid catalyst, and it is unclear if the solid acid contributes any catalytic effect.

Chapter 5: Conclusions and Recommendations

In conclusion, this study has shown that that (chloromethyl)polystyrene catalysts and their sulfonated derivatives leach chloride anions, forming aqueous homogenous acid *in-situ*. Sulfonic acid groups do not appear to be effected under reaction conditions, but chloride groups are hydrolyzed from the surface of the catalyst beads. The generation of liquid acid can be modeled as a first order reaction, yielding the $[H^+]$ concentration as a function of time.

Kinetic modeling was used to investigate the method of catalysis. Homogenous acid catalyzed kinetic parameters along with a reaction mechanism was taken from literature and used to define a set of differential equations that described the system. These differential equations were solved using the $[H^+]$ concentration as a function of time. Additionally, a Monte Carlo method was employed to incorporate experimental uncertainties of the $[H^+]$ concentration and temperature into the kinetic model.

Experimental cellulose hydrolysis data shows good alignment with the liquid acid catalyzed kinetic model. This indicates the reaction is likely catalyzed by the leached homogenous acid, rather than the solid acid catalyst as previously thought.

Future studies would need to acquire more experimental data for cellulose hydrolysis at various time points, to confirm experimental alignment with the kinetic model. Additionally, temperature profiling should be done to determine the exact temperature range of possible within the reactor. Lastly, a fully sulfonated catalyst should be synthesized and tested, to see if there is any catalytic effects from just the sulfonic acid groups.

References

1. U.S Energy Information Administration. “Short-Term Energy Outlook (STEO) Forecast Highlights.” (2017): n. pag. Print.
2. Cefic. “Facts and Figures of the European Chemical Industry 2016.” (2016): n. pag. Print.
3. Zalasiewicz, Jan et al. “The New World of the Anthropocene.” *Environmental Science & Technology* 44.7 (2010): 2228–2231. Print.
4. Hoekman, S. Kent. “Biofuels in the U.S. - Challenges and Opportunities.” *Renewable Energy* 34.1 (2009): 14–22. Web.
5. Nielsen, Rudi P., Göran Olofsson, and Erik G. Søgaard. “CatLiq - High Pressure and Temperature Catalytic Conversion of Biomass: The CatLiq Technology in Relation to Other Thermochemical Conversion Technologies.” *Biomass and Bioenergy* 39 (2012): 399–402. Web.
6. Fendt, Sebastian et al. “Comparison of Synthetic Natural Gas Production Pathways for the Storage of Renewable Energy.” *Wiley Interdisciplinary Reviews: Energy and Environment* 5.3 (2016): 327–350. Web.
7. Balan, Venkatesh. “Current Challenges in Commercially Producing Biofuels from Lignocellulosic Biomass.” *ISRN Biotechnology* 2014.i (2014): 1–31. Web.
8. Hong, Yan et al. “Impact of Cellulase Production on Environmental and Financial Metrics for Lignocellulosic Ethanol.” *Biofuels, Bioproducts and Biorefining* 7.3 303–313. Web.
9. Humbird, D. et al. “Process Design and Economics for Biochemical Conversion of Lignocellulosic Biomass to Ethanol: Dilute-Acid Pretreatment and Enzymatic Hydrolysis of Corn Stover.” *Renewable Energy* 303.May (2011): 147. Web.
10. Rinaldi, Roberto, and Ferdi Schuth. “Acid Hydrolysis of Cellulose as the Entry Point into Biorefinery Schemes.” *ChemSusChem* 2.12 (2009): 1096–1107. Web. 5 Oct. 2017.
11. Chaturvedi, Venkatesh, and Pradeep Verma. “An Overview of Key Pretreatment Processes Employed for Bioconversion of Lignocellulosic Biomass into Biofuels and Value Added Products.” *3 Biotech* 3.5 (2013): 415–431. Web.
12. Huang, Yao-Bing, and Yao Fu. “Hydrolysis of Cellulose to Glucose by Solid Acid Catalysts.” *Green Chem.* 15.5 (2013): 1095–1111. Web.
13. Shuai, Li, and Xuejun Pan. “Hydrolysis of Cellulose by Cellulase-Mimetic Solid Catalyst.” *Energy & Environmental Science* 5.5 (2012): 6889. Web.
14. Scott, David Sanborn. “Fossil Sources: ‘running Out’ is Not the Problem.” *International Journal of Hydrogen Energy* 30.1 (2005): 1–7. Web.
15. Höök, Mikael, and Xu Tang. “Depletion of Fossil Fuels and Anthropogenic Climate Change-A Review.” *Energy Policy* 52 (2013): 797–809. Web.
16. Olah, George A., G. K.Surya Prakash, and Alain Goeppert. “Anthropogenic Chemical Carbon Cycle for a Sustainable Future.” *Journal of the American Chemical Society* 133.33 (2011): 12881–12898. Web.
17. “The Carbon Cycle in the Earth System.” Max Planck Society, www.mpg.de/19314/carbon_cycle.
18. “Biomass Energy Basics.” Biomass Energy Basics | NREL, www.nrel.gov/workingwithus/re-biomass.html.
19. T, Werpy., and Petersen. G. “Top Value Added Chemicals from Biomass Volume I — Results of Screening for Potential Candidates from Sugars and Synthesis Gas Top Value Added Chemicals From Biomass Volume I : Results of Screening for Potential Candidates.” 1 (2004): n. pag. Print.
20. Renewable Energy Sources - Energy Explained, Your Guide To Understanding Energy - Energy Information Administration, www.eia.gov/energyexplained/?page=renewable_home.
21. Singh, Anoop et al. “Key Issues in Life Cycle Assessment of Ethanol Production from Lignocellulosic Biomass: Challenges and Perspectives.” *Bioresource Technology* 101.13 (2010): 5003–5012. Web.
22. OSullivan, A C. “Cellulose: The Structure Slowly Unravels.” *Cellulose* 4.3 (1997): 173–207. Web.

23. Xu, Zhaoyang, and Fang Huang. “Pretreatment Methods for Bioethanol Production.” Applied biochemistry and biotechnology 174.1 (2014): 43–62. Web.
24. Hara, Michikazu, Kiyotaka Nakajima, and Keigo Kamata. “Recent Progress in the Development of Solid Catalysts for Biomass Conversion into High Value-Added Chemicals.” *Science and Technology of Advanced Materials* 16.3 (2015): 1–22. Web.
25. Yang, Qiang, and Xuejun Pan. “Synthesis and Application of Bifunctional Porous Polymers Bearing Chloride and Sulfonic Acid as Cellulase-Mimetic Solid Acids for Cellulose Hydrolysis.” *Bioenergy Research* 9.2 (2016): 578–586. Web.
26. “Microkinetic Modeling.” Microkinetic Modeling | Schmidt Group, schmidt.chem.wisc.edu/microkinetic-modeling.
27. Steinfeld, Jeffrey I., et al. Chemical Kinetics and Dynamics. Prentice Hall, 1999.
28. SriBala, G., and R. Vinu. “Unified Kinetic Model for Cellulose Deconstruction via Acid Hydrolysis.” Industrial and Engineering Chemistry Research 53.21 (2014): 8714–8725. Web.
29. Yan, Lishi et al. “A Comprehensive Mechanistic Kinetic Model for Dilute Acid Hydrolysis of Switchgrass Cellulose to Glucose, 5-HMF and Levulinic Acid.” *RSC Advances* 4.45 (2014): 23492. Web.
30. Garcés, Diego, Eva Díaz, and Salvador Ordóñez. “Aqueous Phase Conversion of Hexoses into 5-Hydroxymethylfurfural and Levulinic Acid in the Presence of Hydrochloric Acid: Mechanism and Kinetics.” *Industrial and Engineering Chemistry Research* 56.18 (2017): 5221–5230. Web.
31. Weingarten, Ronen et al. “Kinetics and Reaction Engineering of Levulinic Acid Production from Aqueous Glucose Solutions.” *ChemSusChem* 5.7 (2012): 1280–1290. Web.
32. Zuo, Yong, Ying Zhang, and Yao Fu. “Catalytic Conversion of Cellulose into Levulinic Acid by a Sulfonated Chloromethyl Polystyrene Solid Acid Catalyst.” *ChemCatChem* 6.3 (2014): 753–57.Web.
33. Tyufekchiev, Maksim et al. “Cellulase-Inspired Solid Acids for Cellulose Hydrolysis: Structural Explanations for High Catalytic Activity.” *ACS Catalysis* 8.2 (2018): 1464–1468. Web.
34. Lambert, Joseph B. *Organic Structural Spectroscopy*. Upper Saddle River, NJ: Prentice Hall, 1998. Print.
35. Saeman, Jerome F. “Kinetics of Wood Saccharification - Hydrolysis of Cellulose and Decomposition of Sugars in Dilute Acid at High Temperature.” *Industrial & Engineering Chemistry* 37.1 (1945): 43–52. Web.
36. “ode45.” Solve Nonstiff Differential Equations - Medium Order Method - MATLAB ode45, www.mathworks.com/help/matlab/ref/ode45.html.

Appendix A: Matlab Code

```
% Kinetic Model for Acid Catalyzed Hydrolysis of Cellulose based on
% Saeman and Weingarten et al. w/ Hplus concentration changing over
time,
% variable T, and variable H+

clear; clc; close all;

CellMW = 162.1406; %g/mol MW of cellulose

% Reaction Conditions
R = 8.314E-3;
WeightCellulose = 0.1; %Initial weight (g) of cellulose in reactor
VolumeWater = 2/1000; %Initial volume of water in reactor in L
CelluloseO = WeightCellulose/VolumeWater/CellMW;

Hpluslb = 0.11;%Lower Bound H+
Hplusub = 0.16;%Upper Bound H+
h = @(r) Hpluslb + (Hplusub-Hpluslb)*r;%Pre-exponential factor for time
dependent H+ equation w/ variability given by standard deviation

%CHplus = @(t,r) h(r)*(1-exp(-0.007435*t)); %CHplus concentration based
on CMP model (between 0.03 to 0.06)
CHplus = @(t,r) h(r)*(1-exp(-0.00708333*t)); %CHplus concentration
based on CMP-0.3 model (between 0.11 to 0.16)

Xintermediate = @(t,r) CHplus(t,r)*(98.079/2); %Convert mole H+ to
grams H2SO4
Yintermediate = @(t,r) Xintermediate(t,r)*(1/1.84); %Convert grams
H2SO4 to mL H2SO4
Zintermediate = @(t,r) (1000-Yintermediate(t,r))*(0.99823); %Convert
remaining L to g of water

Hpluswt = @(t,r)
(Xintermediate(t,r)/(Xintermediate(t,r)+Zintermediate(t,r)))*100; %wt
of HCl/wt HCl + wt H2O(H+ given as a wt % of H2SO4)

Tlb = 273+167;%Lower Bound Temperature
Tub = 273+175;%Upper Bound Temperature
T = @(a) Tlb + (Tub-Tlb)*a;

k1 = @(t,a,r) 1.73E19*(Hpluswt(t,r)^1.34)*10^(-(179.5/(2.303*R*T(a))));

% Hydrolysis of Cellulose to Glucose and Decomosition Products

A2o = 10^18.44;
A3o = 10^3.86;
A4o = 10^11.50;
A5o = 10^16.83;

Ea2 = 160.16;
```

```
Ea3 = 50.68;
Ea4 = 94.72;
Ea5 = 141.94;

m2 = 1.290;
m3 = 2.764;
m4 = 1.176;
m5 = 1.176;

Hx2 = 0;
Hx3 = 0.29;
Hx4 = 0;
Hx5 = 0;

A2 = @(t,r) A2o*(Hx2+CHplus(t,r)^m2);
A3 = @(t,r) A3o*(Hx3+CHplus(t,r)^m3);
A4 = @(t,r) A4o*(Hx4+CHplus(t,r)^m4);
A5 = @(t,r) A5o*(Hx5+CHplus(t,r)^m5);

k2 = @(t,r,a) (A2(t,r))*exp(-Ea2/(R*T(a)));
k3 = @(t,r,a) (A3(t,r))*exp(-Ea3/(R*T(a)));
k4 = @(t,r,a) (A4(t,r))*exp(-Ea4/(R*T(a)));
k5 = @(t,r,a) (A5(t,r))*exp(-Ea5/(R*T(a)));

n = 25;
a = rand(n,1);
r = rand(n,1);

tspan = linspace(0, 600, 601);
fun1 = @(t,z,r,a) [-(k1(t,r,a)*z(1));(k1(t,r,a)*z(1))-(k2(t,r,a)*z(2))-
(k3(t,r,a)*z(2));(k2(t,r,a)*z(2))-(k4(t,r,a)*z(3))-
(k5(t,r,a)*z(3));(k4(t,r,a)*z(3))];

%Solving system of ODEs
for iter1 = 1:length(a)
    for iter2 = 1:length(r)
    [t,z] = ode45(@(t,z) fun1(t,z,a(iter1),r(iter2)),tspan,[CelluloseO
0 0 0]);
    tz1(iter1,iter2,:,:) = [t  z];
    end
end

%%

%Plotting results
for x = 1:n
    for y = 1:n
        figure(1)
        hold on
        grid on
        time = tz1(x,y,:,1);
        time1 = squeeze(time);
        Cell = tz1(x,y,:,2);
        Cell1 = squeeze(Cell);
        Gluc = tz1(x,y,:,3);
        Gluc1 = squeeze(Gluc);
```

```
        HMF = tz1(x,y,:,4);
        HMF1 = squeeze(HMF);
        LA = tz1(x,y,:,5);
        LA1 = squeeze(LA);

        Cellconv = ((CelluloseO - Cell1)/CelluloseO)*100;
        Gyield = (Gluc1/CelluloseO)*100;
        HMFyield = (HMF1/CelluloseO)*100;
        LAyield = (LA1/CelluloseO)*100;

        %plot(t,Cellconv,'b',t,Gyield,'g',t,HMFyield,'k',t,LAyield,'m')
        plot(t,Gyield,'b',t,HMFyield,'k',t,LAyield,'m')
        end
end
hold on

legend('Glucose','HMF','Levulinic/Formic Acid','Location','best')

%Actual cellulose hydrolysis experimental data collected by Maksim
realx = 600;
realcmpG = 13.6;
realcmpGstd = 5.2;
realcmpFA = 20.3;
realcmpFAstd = 9.3;

realcmp3G = 6.3;
realcmp3Gstd = 2.5;
realcmp3FA = 50.9;
realcmp3FAstd = 4.1;

hold on
errorbar(realx,realcmp3G,realcmp3Gstd,'ko','MarkerEdgeColor','k','Marke
rFaceColor','b','MarkerSize',8)
errorbar(realx,realcmp3FA,realcmp3FAstd,'ko','MarkerEdgeColor','k','Mar
kerFaceColor','m','MarkerSize',8)
set(gca,'FontSize',14)
xlabel('Time (min)','fontsize',16), ylabel('% Yield','fontsize',16)
axis([0 600 0 60])
```

Appendix B: CMP Raw Data

CMP				
Time (hr)	Trial	Mass Polymer (g)	Mass Water (g)	pH
0.5	1	0.1927	1.9906	1.87
	2	0.1953	1.9874	2.04
	3	0.2070	1.9781	2.23
1	1	0.2068	2.0060	1.80
	2	0.2061	1.9992	1.80
	3	0.2057	2.0030	1.89
2	1	0.1950	2.0070	1.44
	2	0.2079	2.0072	1.54
	3	0.2058	2.0368	1.48
4	1	0.2064	2.0011	1.60
	2	0.2006	2.0038	1.32
	3	0.2066	1.9856	1.52
6	1	0.1911	2.0221	1.55
	2	0.2047	2.0069	1.36
	3	0.2019	1.9980	1.38
8	1	0.1999	2.0090	1.43
	2	0.2052	2.0017	1.30
	3	0.2030	2.0079	1.43
10	1	0.2001	n/a	1.60
	2	0.2058	n/a	1.39
	3	0.1984	n/a	1.58
	1	0.2042	2.0025	1.27
	2	0.2058	2.0035	1.20
	3	0.2016	1.9994	1.22

	[Cl-]					
Time (hr)	Weight Sample (g)	Total Weight (g)	Peak Area	Diluted Conc. (ppm)	Undiluted Conc. (ppm)	Conc. (M)
0.5	0.0961	35.8608	8.241	1.6027	598.0595476	1.68E-02
	0.0946	35.8717	7.086	1.3781	522.5524619	1.47E-02
	0.0950	36.0940	5.255	1.0220	388.2862904	1.09E-02
1	0.0924	35.9597	17.344	3.3730	1312.687293	3.69E-02
	0.0937	35.6688	18.250	3.5492	1351.075766	3.80E-02
	0.0947	35.5361	13.302	2.5869	970.7438672	2.73E-02
2	0.0955	35.6124	20.587	4.0037	1492.996754	4.20E-02
	0.0955	35.7187	16.208	3.1521	1178.934368	3.32E-02
	0.0931	35.5136	15.505	3.0154	1150.230068	3.24E-02
4	0.0946	35.4224	15.313	2.978	1115.094156	3.14E-02
	0.0962	35.4546	22.843	4.443	1637.287531	4.61E-02
	0.0952	35.8273				
6	0.0949	35.9860	15.584	3.0307	1149.249254	3.23E-02
	0.0953	35.8916	22.068	4.2917	1616.332931	4.55E-02
	0.0972	35.6072	22.198	4.3170	1581.442237	4.45E-02
8	0.0960	35.9158				
	0.0967	35.1090	32.903	6.3989	2323.247138	6.54E-02
	0.0947	36.8890	25.261	4.9127	1913.662603	5.38E-02
10	0.0955	35.9416	72.938	14.1848	5338.45779	1.50E-01
	0.0915	35.0550	88.298	17.1719	6578.814966	1.85E-01
	0.0952	35.1967	138.084	26.8541	9928.331852	2.79E-01

Appendix C: CMP-SO_3H-0.3 Raw Data

CMP-SO3H-0.3				
Time (hr)	Trial	Mass Polymer (g)	Mass Water (g)	pH
0.5	1	0.2044	2.0077	1.31
	2	0.2009	2.0078	1.35
	3	0.2037	2.0104	1.35
1	1	0.2014	1.9983	1.24
	2	0.2012	2.0064	1.23
	3	0.2004	2.0086	1.27
2	1	0.2024	2.0126	1.04
	2	0.2014	2.0116	1.02
	3	0.2046	2.0072	1.10
4	1	0.2030	2.0114	1.07
	2	0.2071	2.0211	0.96
	3	0.2065	2.0056	0.97
6	1	0.2005	2.0186	0.85
	2	0.2041	2.0210	0.96
	3	0.2006	2.0124	0.91
8	1	0.2041	1.9944	0.80
	2	0.2009	2.0181	0.89
	3	0.2014	2.0111	0.96
10	1	0.2066	2.0017	1.00
	2	0.2048	2.0021	1.01
	3	0.2032	1.9993	0.89

[Cl-]					
Time (hr)	Weight Sample (g)	Total Weight (g)	Diluted Conc. (ppm)	Undiluted Conc. (ppm)	Conc. (M)
0.5	0.0954	49.5773	3.3562	1744.143965	4.91E-02
	0.0945	50.3270	3.1329	1668.459876	4.69E-02
	0.0945	51.1358	3.0901	1672.113604	4.70E-02
1	0.0867	50.5258	4.3635	2542.898827	7.15E-02
	0.0946	50.8939	5.5408	2980.897686	8.39E-02
	0.0948	51.2282	4.9959	2699.693717	7.59E-02
2	0.0943	50.4947	7.3539	3937.783397	1.11E-01
	0.0948	50.3734	6.5712	3491.705549	9.82E-02
	0.0943	50.4499	7.0790	3787.219959	1.07E-01
4	0.0950	50.0159	9.9884	5258.724374	1.48E-01
	0.0950	50.0328	10.6458	5606.728234	1.58E-01
	0.0941	50.1227	10.5957	5643.837326	1.59E-01
6	0.0949	50.2381	9.8945	5237.943946	1.47E-01
	0.0940	50.3313	10.0363	5373.830066	1.51E-01
	0.0778	50.4259	7.2189	4678.914261	1.32E-01
8	0.0940	50.0848	11.0277	5875.746266	1.65E-01
	0.0925	51.5559	9.9891	5567.535575	1.57E-01
	0.0924	50.2604	9.9468	5410.499423	1.52E-01

[SO4-2]					
Time (hr)	Weight Sample (g)	Total Weight (g)	Diluted Conc. (ppm)	Undiluted Conc. (ppm)	Conc. (M)
0.5	0.0954	49.5773	0.3310	172.0134832	1.79E-03
	0.0945	50.3270	0.3200	170.4194709	1.77E-03
	0.0945	51.1358	0.3193	172.7794808	1.80E-03
1	0.0867	50.5258	0.3899	227.2204085	2.37E-03
	0.0946	50.8939	0.6611	355.6655105	3.70E-03
	0.0948	51.2282	0.4602	248.6837304	2.59E-03
2	0.0943	50.4947	0.7359	394.0514287	4.10E-03
	0.0948	50.3734	0.5630	299.1584831	3.11E-03
	0.0943	50.4499	0.6373	340.9514451	3.55E-03
4	0.0950	50.0159	1.0606	558.3880373	5.81E-03
	0.0950	50.0328	2.0035	1055.165419	1.10E-02
	0.0941	50.1227	1.4741	785.1846129	8.17E-03
6	0.0949	50.2381	0.9399	497.5636479	5.18E-03
	0.0940	50.3313	1.0104	541.0079311	5.63E-03
	0.0778	50.4259	0.6718	435.4257021	4.53E-03
8	0.0940	50.0848	1.1977	638.1549464	6.64E-03
	0.0925	51.5559	1.2352	688.4524074	7.17E-03
	0.0924	50.2604	1.0015	544.7596385	5.67E-03